

1 **PLACER PLATINUM-GROUP MINERALS IN THE SHETLAND OPHIOLITE**  
2 **COMPLEX DERIVED FROM ANOMALOUSLY ENRICHED PODIFORM**  
3 **CHROMITITES.**

4  
5 Prichard, H.M.<sup>1</sup>, Suárez, S.<sup>1,2</sup>, Fisher, P.C.<sup>1</sup>, Knight, R.D.<sup>1</sup> & Watson, J.S.<sup>3</sup>

6  
7 <sup>1</sup>School of Earth and Ocean Sciences, Cardiff University, Main College, Park Place, Cardiff, CF10 3AT, UK.

8 <sup>2</sup> Department of Mineralogy and Petrology, UPV/EHU, 48940 Leioa & Ikerbasque, 48011 Bilbao, Spain.

9 <sup>3</sup>Open University, Department of Environment, Earth and Ecosystems, Walton Hall, Milton Keynes,  
10 Buckinghamshire, MK7 6AA, UK.

11 ✉ Email: saioa.suarez@ehu.es

12  
13  
14 **Abstract.** Highly anomalous platinum-group element (PGE) concentrations in the podiform  
15 chromitites at the Cliff and Harold's Grave localities in the Shetland ophiolite complex have  
16 been well documented previously. The focus of this study is alluvial platinum-group minerals  
17 (PGM) located in small streams that drain from the PGE-rich chromitites. The placer PGM  
18 assemblage at Cliff is dominated by Pt-arsenides (64%) and Pd-antimonides (17 %), with less  
19 irarsite–hollingworthite (11%) and minor Pd-sulfides, Pt-Pd-Cu and Pt-Fe alloys, and laurite.  
20 Gold also occurs with the PGM. Alluvial PGM have average sizes of 20 x 60 µm, with  
21 sperrylite the largest grain identified at 110 µm in diameter, matching the range reported for  
22 the primary PGM in the source rocks. The placer assemblage contains more Pt-bearing and  
23 less Pd-bearing PGM compared with the rocks. The more resistant sperrylite and irarsite–  
24 hollingworthite grains which are often euhedral become more rounded further downstream  
25 whereas the less resistant Pd-antimonides which are commonly subhedral may become  
26 striated and etched. Less stable phases such as Pt- and Pd-oxides and other Ni-Cu-bearing  
27 phases located in the rocks (i.e. Ru-pentlandite, PtCu, Pd-Cu alloy) are absent in the placer  
28 assemblage. Also the scarce PGM (PdHg, Rh- and Ir-Sb) and Os in the rocks are absent. At  
29 Harold's Grave only 3 alluvial PGM (laurite, Ir, Os) and Au were recovered reflecting the

30 limited release of IPGM from chromite grains in the rocks. In this cold climate with high  
31 rainfall, where erosion dominates over weathering, the PGM appear to have been derived  
32 directly from the erosion of the adjacent PGE-rich source rocks and there is little evidence of  
33 in situ growth of any newly formed PGM. Only the presence of dendritic pure Au and Pd-,  
34 Cu-bearing Au covers on the surface of primary minerals may indicate some local  
35 reprecipitation of these metals in the surficial conditions.

36 **Keywords:** Shetland ophiolite complex, Cliff, Harold's Grave, alluvial concentrates,  
37 platinum-group minerals, platinum-group elements.

38

## 39 **Introduction**

40 There are many examples of placer PGM around the world as summarised in Cabri et al.  
41 (1996) and Weiser (2002). Placer PGM exhibit variable shapes, commonly form flakes or are  
42 rounded or knobbly, and more than 90% of placer PGM are alloys of Pt-Fe and Os-Ir-Ru-Pt.  
43 Ophiolitic placer PGM tend to be dominated by Os-Ir-Ru alloys (Cabri et al., 1996).

44

45 There is a long standing debate about whether placer PGM erode mechanically from PGE-  
46 bearing rocks or whether they grow in situ in stream banks draining from PGE-bearing  
47 sources. One of the main lines of evidence for mechanical erosion comes from PGM nuggets  
48 that contain inclusions of igneous silicates and exotic PGM that may have been preserved in  
49 the matrix of the nuggets. Commonly, placer nuggets are much bigger than the PGM in the  
50 source rocks. The argument here is that large PGM in the streams represent the few large  
51 PGM concentrated from extensive erosion of the host rocks (Cabri and Harris, 1975) and are  
52 overlooked in geochemical and petrological surveys. The alternative view is that placer  
53 nuggets may grow in situ in streams. Destruction of PGM by weathering and erosion of the  
54 host rocks would liberate the PGE, which may travel downstream in solution and re-

precipitate due to changes in the geochemistry of the PGE-bearing solutions (e.g. Bowles, 1986; Bowles et al., 2000). PGM in the host rocks often show evidence of being broken down and oxidised as they weather (Bowles et al., 2017a), thus destroying the PGM for later re-precipitation in the streams. The secondary precipitation of placer PGM has been evidenced by reworking and concentric growths (e.g. Cabral et al., 2009; Zaccarini et al., 2013), or by delicate arrangements of PGM (e.g. Bowles et al., 2017b) inconsistent with pervasive mechanical and hydraulic erosion of the grains.

62

Podiform chromitites in ophiolite complexes are typically enriched in IPGE (Ir, Ru, Os) over PPGE (Pt, Pd, Rh) and are characterized by Ru–Os–Ir-dominant PGM (IPGM), mainly laurite–erlichmanite ( $\text{RuS}_2$ – $\text{OsS}_2$ ), irarsite ( $\text{IrAsS}$ ), and Os–Ir–Ru alloys. Relevant examples are compiled, for example, in Prichard and Brough (2009) and O'Driscoll and González-Jiménez (2016). Some other ophiolitic chromitites are however significantly enriched in PPGE and contain Pt-, Pd-, and Rh-bearing minerals (PPGM), e.g. sperrylite ( $\text{PtAs}_2$ ), stibiopalladinite ( $\text{Pd}_5\text{Sb}_2$ ), isoferroplatinum ( $\text{Pt}_3\text{Fe}$ ), cooperite–braggite ( $\text{PtS}$ – $\text{PdS}$ ), and Pt–Pd–Rh±base-metal alloys (González-Jiménez, 2014). Some well known examples are chromitites from Thetford Mines (Corrivaux and Laflamme, 1990) and Newfoundland (Baie Verte Peninsula; Escayola et al., 2011) in Canada, Leka in Norway (Pedersen et al., 1993), Cabo Ortegal in Spain (Moreno et al., 1999, 2001), Bragança in Portugal (Bridges et al., 2013), Albanian ophiolites (Ohnenstetter et al., 1999), Pindos in Greece (Grammatikopoulos et al., 2007; Prichard et al., 2008a), Berit in Turkey (Kozlu et al., 2014), Al'Ays in Saudi Arabia (Prichard et al., 2008b), Acoje in the Philippines (Bacuta et al., 1988; Orberger et al., 1988) and Pirogues in New Caledonia (Augé et al., 1998).

78

79 The Shetland ophiolite situated on Unst, the most northerly of the Shetland Islands, northeast  
80 of Mainland Scotland, was one of the first ophiolite complexes found to contain chromitites  
81 enriched in both IPGM and PPGM, with all six PGE being present at ppb or ppm levels  
82 (Prichard et al., 1986). The history of their discovery is described in Brough et al. (2015).  
83 Prichard et al. (2008b) and Prichard and Brough (2009) concluded that the PPGE-rich  
84 chromitites in ophiolites formed from magmas that were close to sulfide liquid saturation,  
85 resulting in the local accumulation of traces of strongly PGE-enriched sulfide liquid.

86

87 The Shetland ophiolite consists of mantle harzburgite overlain by crustal dunite, wehrlite,  
88 pyroxenite and gabbro, with a few dykes intruded into the gabbro at the top of the sequence  
89 (Fig. 1) (Prichard, 1985; Flinn, 1985). The mantle and crustal ultramafics contain  
90 disseminated chromite and there are a number of podiform chromitites in the mantle that are  
91 surrounded by an envelope of dunite enclosed in harzburgite. Not all of these pods are  
92 enriched in PGE with concentrations of only 10-100 ppb. The exceptions are localities at  
93 Cliff and Harold's Grave where enrichment is at ppm levels (up to ~58 and 14 ppm total PGE,  
94 respectively). The Cliff locality is enriched in all six PGE and is the main focus of this study  
95 whereas the Harold's Grave locality is enriched in IPGE (Prichard and Brough, 2009).

96

97 There have been a number of studies of the PGM in the Shetland ophiolite. Generally the  
98 PGM in the chromitites are characterised by euhedral Os-Ir-bearing laurite included within  
99 the chromite grains and Os-Ir-barren laurite of irregular shape where the laurite is in contact  
100 with the serpentine interstitial to the chromite grains. This interstitial laurite is often  
101 accompanied by native Os, irarsite and ruthenian pentlandite (Prichard et al., 1986; Tarkian  
102 and Prichard, 1987; Prichard et al., 1994). Occasional composite grains consisting of more  
103 varied PGM do, however, occur as for example in the chromitite pod at Nikkavord North,

South Cliff, which consists of laurite, irarsite, hollingworthite (RhAsS), ruthenian pentlandite, Ni-Rh antimonide and native Os (Prichard et al., 1986). The PGM assemblage in the overlying crustal dunite, wehrlite and pyroxenite sequence contain IPGM in discontinuous chromite layers and PPGM in adjacent sulfide-bearing dunite including Pt-, Pd-rich stibiopalladinite, geversite (PtSb<sub>2</sub>), genkinitite ((Pt,Pd)<sub>4</sub>Sb<sub>3</sub>), Pt-Fe-Cu alloys and Pt- and Pd-oxides and ochres, which are low-reflectance minerals formed during the alteration of earlier PGM (Prichard et al., 1994). The wehrlite contains a mineral assemblage formed from a more fractionated magma consisting of Pd-Cu sulfide and Pd-Pb alloys ±Pt and ±Au in unaltered clinopyroxenite, with Pt and Pd arsenides, antimonides and tellurides in adjacent serpentine (Prichard et al., 1994). The PGM located in different stratigraphic levels and in the different chromitite pods within the mantle have been summarised in Prichard et al. (1994).

The present study focuses on the two PGE-rich localities of the Shetland ophiolite, Cliff and Harold's Grave. Both are disused chromite quarries located in the north of the ophiolite and consist of several *en echelon* chromitite (also including chromite-rich lenses with >10% chrome-spinel, normally 50-90%) enclosed by a dunite envelope in mantle harzburgite. Cliff is near the basal thrust (Fig. 2) and has a dunite envelope smaller than Harold's Grave. Chromitite lenses at both localities are up to 10 m long and 1 m wide (Prichard et al., 1988). PGM in the Cliff and Harold's Grave chromitites are described in Prichard and Tarkian (1988) and Tarkian and Prichard (1987). These authors observed that IPGM are often enclosed in chromite whereas PPGE-bearing PGM occur within the serpentinised silicate matrix and are predominantly interstitial to the chromite grains.

PGM at Harold's Grave are dominated by laurite, ruthenian pentlandite, native Os and irarsite often rimmed by hollingworthite. Other minerals recorded include genkinitite, hongshiite

(PtCu), stibiopalladinite and unnamed Rh-Sb-S and Rh-Ni-Sb phases (Prichard and Tarkian, 1988). Recent studies reveal up to five generations of PGM in these chromitites (Prichard et al., 2017). In contrast, the PGM in the rocks at Cliff are PPGM dominated. A PPGM assemblage occurs in sulfide-bearing dunites adjacent to the chromitites which contain IPGM. The very enriched PPGM-bearing dunite with disseminated chromite is thought to have been hydrothermally upgraded during the introduction of As and Sb, at a late stage as the ophiolite was emplaced (Prichard and Lord, 1993; Lord et al., 1994). In this alteration assemblage all six PGE form PGM in chromite-rich dunites at Cliff. The PGM consist of sperrylite, Pd-antimonides, members of the irarsite–hollingworthite solid solution series, Pt-Pd-Au-Cu alloys, laurite, native Os, potarite (PdHg) and Pt- and Pd-oxides, with PGM diameters up to 30  $\mu\text{m}$ , all accompanied by ruthenian pentlandite. Other studies have been undertaken on the Cliff PGM as for example by Derbyshire et al. (2012) who located mainly sperrylite.

The aim of this investigation was to examine the streams draining the Cliff and Harold's Grave sites to characterise the placer PGM present and assess their genesis. The placer PGM are compared to the primary PGM in the source rocks, and variations in the former with increasing distance from the source rocks are also assessed. This study shows for the first time the PGM in the streams draining the Shetland ophiolite and contributes to the increasing knowledge base regarding whether alluvial PGM are mechanically eroded from their source rocks, or whether they precipitate in situ as a result of chemical weathering.

## **Methods**

A small network of streams with a maximum width of 0.5 m drains the ponds in the disused chromite quarries at Cliff. These then coalesce to discharge into the Loch of Cliff, 400 m to

the west of the Cliff quarries (Fig. 2). Rock samples were taken at the quarries and samples of sediments were collected from the streams at four separate locations (Figs. 2 and 3; Table 1) and panned on site in a plastic pool. Four samples (C2–C5) were taken from the first location, at the commencement of the stream from the quarry pond. Sample C2 was taken at the immediate exit of the pond whereas samples C3–C5 were within 5 m of the Cliff quarries. A further four samples (C6–C9) were collected from the second location consisting of meanders 20–50 m downstream of the quarries. Another three samples (C10–C12) were taken downstream within 20–30 m of the exit of the meander zone and after a moderate increase in the slope gradient. Lastly, samples were collected from the stream as it plunged over the basal thrust of the ophiolite (CS).

Sampling at Harold's Grave was conducted over a sloping E–W section spanning about 20 m along a stream draining outcrops of dunite cut by discontinuous layers of chromitite (Table 2). The section starts below a disused PGE-rich quarry and sampling included ten sites separated by three natural ponds, the first two aligned at the beginning of the section and the last one situated further down slope. The first five samples (HG1–HG5) were taken from the entrance and exit of the first two ponds. This area is largely covered by vegetation; it has a 10 cm topsoil with a high concentration of organic matter followed by a subsoil layer of significantly weathered rock. The soil produced negligible heavy concentrates and holes were excavated to a depth of 15–20 cm to obtain samples. The next four samples (HG6–HG9) were collected from a site with more outcrop of fractured dunite following a strong break of slope with increasing gradient. The last sample (HG10) was taken from the exit of the most distal pond, where the soil layer becomes thicker again. Overall, the dense fraction recovered from sampling sites at Harold's Grave was much smaller than that recovered from Cliff.

Panned size fractions below 150  $\mu\text{m}$  were examined for precious metal minerals and PGM using a Cambridge Instruments (ZEISS NTS) S360 scanning electron microscope (SEM), coupled to an Oxford Instruments INCA energy plus energy dispersive X-ray analytical system (EDX) at Cardiff University. Qualitative analyses were obtained of the mineral surfaces, and polished blocks were utilized for fully quantitative analyses (Table 3). Operating conditions for the quantitative analyses consisted of a 20 kV accelerating voltage, 1 nA beam current and fixed beam size (approximately 10-15 nm), with a live-time of 50 s for EDX. A cobalt reference standard was regularly analyzed, in order to check for any drift in the analytical conditions. A comprehensive set of standards obtained from MicroAnalysis Consultants Ltd. (St Ives, Cambridgeshire) was used to calibrate the EDX analyzer.

## **Results**

### ***Alluvial PGM at Cliff***

A total of 108 PGM and 8 grains of gold have been identified in samples C3–C11 and CS collected from the streams at Cliff (Fig. 4a, Table 1). The PGM assemblage consists mainly of sperrylite (69 grains; 64% abundance), Pd-antimonides (18 grains; 17%) and members of the irarsite–hollingworthite solid-solution series (11 grains; 11%). Less abundant phases are Pd-sulfides (4 grains; 4%), and Pt-alloys, Pd-arsenide and laurite (6 grains in total; 6%). These PGM range in size from 8-110  $\mu\text{m}$  and consist of single minerals as well as composite grains. The placer PGM reflect those observed in the source rocks, but exhibit less variety (Fig. 4a, Table 1). Quantitative analyses of polished surfaces of the typical PGM have been completed (Table 3).

Alluvial PGM in the streams at Cliff occur only within the first 100-150 m from the disused quarries (Fig. 2; Fig. 4b). Of the 108 PGM grains recovered, 22% are from the exit of the



main pond close to the quarries, 58% are from the meander zone about 50 m away from the quarries, and 19% come from downstream of the meander exit, about 100 m away. However, only one PGM grain was recovered further downstream, where the stream plunges over the basal thrust. The type, abundance and size of the alluvial PGM do not vary significantly downstream (Table 1, Fig. 4b). Sperrylite, Pd-antimonides and sulfarsenides together with Pt-alloys and gold occur all along the stream. Pd-sulfides and -arsenides persist closer to the quarries but are not present downstream and laurite, although scarce, appears furthest from the source (Fig. 4b). The main PGM recovered from the streams at Cliff are described next.

### *Sperrylite*

Sperrylite is the most abundant PGM in the streams draining Cliff. It is commonly euhedral to subhedral and occurs in single cubes, octahedrons or aggregates of cubes that are more or less abraded. Single grains range in size from 15 to 110  $\mu\text{m}$  and aggregates reach up to 100  $\mu\text{m}$  across.

Angular sperrylite is more common close to the Cliff quarries (Fig. 5). This sperrylite is often cracked, with pits and furrows on the surface. It occasionally shows surface structures that may correspond to a cleavage (Fig. 5a-c) and it can occur intergrown with silicates preserved from the host rock (Fig. 5d-e), possibly chlorite or serpentine. Many grains of sperrylite show a more jagged and altered appearance with extensive pitting of the mineral surfaces (Fig. 5f-i). Grains or aggregates of euhedral sperrylite show more abraded edges with increasing distance from the quarries (Fig. 5j-l). In fact, about 40% of the sperrylite grains recovered from the streams are subhedral to subrounded (Fig. 6a-l) and occur mainly downstream, further from the quarries.

Sperrylite forms composite grains with irarsite (Fig. 7a-b) and Pd-antimonides (Fig. 7c-d). It also occurs with laurite (Fig. 7e) and with the only grain of Pd-arsenide identified (Fig. 7f), which attains a composition close to  $(\text{Pd,Fe,Ni})_2(\text{As,S})$ . Polished sections of sperrylite reveal other mineral associations (Fig. 8). These include: (i) Pt-alloys of the tetraferroplatinum type (PtFe) in elongate grains 40  $\mu\text{m}$  across that are enclosed in broken sperrylite (Fig. 8a); (ii) ruarsite ( $\text{RuAsS}$ ) at the contact between sperrylite and stibiopalladinite (Fig. 8b); (iii) platarsite ( $\text{PtAsS}$ ) on the edge of abraded sperrylite (Fig. 8c); and (iv) Ni-sulfides and -arsenides (millerite ( $\text{NiS}$ ) – godlevskite ( $\text{Ni}_9\text{S}_8$ ) and nickeline ( $\text{NiAs}$ ), which occur as euhedral or elongated inclusions less than 10  $\mu\text{m}$  long within sperrylite (Fig. 8d).

Sperrylite has a regular  $\text{PtAs}_2$  composition throughout the streams. Occasionally Rh (up to 9 wt.%), and minor amounts of Ru, Pd, Fe or Cu ( $\leq 2$  wt.% each) have been detected. Antimony and S ( $\leq 4$  wt.% each) can replace As (Table 3). This composition is similar to that of sperrylite in the source chromitites, which contain lower but regular Fe ( $<0.5$  wt.%) and Sb concentrations ( $\leq 3$  wt.%) (Prichard and Tarkian, 1988).

#### *Palladium antimonides*

Palladium antimonides are the next most abundant PGM. The size of these PGM ranges from 20 to 105  $\mu\text{m}$  in diameter. They are more altered than the sperrylites in the streams and only 23% of the grains recovered preserve a euhedral shape (Fig. 9a). This occurs normally close to the quarries, where grains are often broken (Fig. 9b-c). Within the meander zone, all the grains show a characteristic fine striation on their surfaces (Fig. 7c; Fig. 9d-g) denoting a lower resistance in the stream compared to sperrylite. The group of grains located at the exit of the meander zone all show an etched appearance (Fig. 9h-i). Polished sections of Pd-antimonide grains are smooth and internal inclusions are not observed. They

typically exhibit homogeneous cores surrounded by an external rim of dismembered Pd-antimonide. Internal fractures are also common (Fig. 8b).

Pd-antimonides often form composite grains with sperrylite (Fig. 7c-d, Fig. 8b), Pd-sulfides (Fig. 9a), and Pt-alloys consisting of Pt-Pd-Cu (Fig. 9c) and PtFe (Fig. 9e). The latter is a tetraferroplatinum included within a Pd-antimonide grain (Fig. 9e). In some cases, Pd-antimonide occurs with electrum (e.g. Fig. 9d) which forms a thin cover along the surface structures of the PGM.

Alluvial Pd-antimonides attain a composition that resembles stibiopalladinite ( $\text{Pd}_{31}\text{Sb}_{12}$ – $\text{Pd}_{5+x}\text{Sb}_{2-x}$ , where  $x=0.04$ ) with some compositions extending towards  $\text{Pd}_5\text{Sb}_3$ , according to ideal Pd-Sb phases of the Pd-Sb-Te system reported by Kim and Chao (1991) (Fig. 10a). Analyses of Pd-antimonides yield elevated Cu contents for most of the analyzed grains (0–5 wt.% Cu; av. 2.7 wt.%), occasional contents of As ( $\leq 3.5$  wt.%) and Ni ( $\leq 0.7$  wt.%), and rare Fe ( $\leq 2.7$  wt.%) (Table 3). No other PGE have been recorded other than Pt. Similar compositions are reported for Pd-antimonides in the host rocks at Cliff (mertieite II – stibiopalladinite, Fig. 10a), although these contain more Pd, and some Pt up to 0.8 wt.% (Prichard and Tarkian, 1988).

### *Sulfarsenides*

End and intermediate members of the irarsite–hollingworthite–platarsite solid solution series have been located throughout the streams draining Cliff.

Irarsite is the most abundant phase (n=6 grains) and occurs in single or composite grains and aggregates with sizes ranging from 30 to 84  $\mu\text{m}$  in diameter. Irarsite in composite grains can

be euhedral (Fig. 7a-b) and aggregates with etched surfaces also preserve the euhedral shape of the grains (Fig. 11a). More often irarsite occurs as subhedral, etched grains (Fig. 11b-c). In two cases it forms composite grains with sperrylite (Fig. 7a-b) and in one case with hollingworthite (Fig. 11c). Alluvial irarsite shows two compositional trends, one with increasing Rh content and the other with increasing Pt content (Fig. 10b). Normally, irarsite attains a (Ir,Rh)AsS composition, with average Rh contents of about 7 wt.% (Table 3). Some Sb is also detected (< 1.5 wt.%). Less often, irarsite contains elevated Pt up to 22 wt.% and Ru up to 10 wt.%. Iridium-end members have not been located in the streams although they are present in the rocks from Cliff (Tarkian and Prichard, 1987; Fig. 10b). Exceptionally, one grain of platarsite (PtAsS) and another of ruarsite (RuAsS) have been located in polished sections of the alluvial PGM. Platarsite occurs on the edge of a sperrylite grain (Fig. 8c, Table 3). Ruarsite is in a polyphase grain with sperrylite and Pd-antimonide and contains elevated Os up to 37 wt.% (Fig. 8b, Table 3). It is of note that irarsite in the rocks from Cliff is unusually Pt poor (Prichard and Tarkian, 1988) whereas Pt-bearing irarsite is observed in the streams (Fig. 10b).

Hollingworthite occurs as subhedral grains (n=5) with sizes from 10 to 80  $\mu\text{m}$  across (Fig. 11c-f). Two of these are single grains (e.g. Fig. 11d) and the other three form composite grains with irarsite (Fig. 11c), Pd-antimonide (Fig. 11e) or gold (Fig. 11f). One grain was identified as end member hollingworthite (RhAsS, Fig. 11d) whereas the others contain Pt ( $\leq$  6 wt.%) and rarely Ir or Os up to 11wt.% and 6 wt.%, respectively. Similarly to irarsite, hollingworthite contains more Pt in the placers than in the source rocks (Fig. 10b).

#### *Less abundant PGM*

303 Palladium sulfides (n=4 grains) occur both as subhedral grains with Pd-antimonides  
 304 close to the disused quarries at Cliff (n=2 grains, Fig. 9a) and as single, broken grains 10–70  
 305  $\mu\text{m}$  long in the meander zone. The two grains close to the quarries resemble vasilite in  
 306 composition  $(\text{Pd, Fe, Cu})_{16}(\text{S, As, Sb})_7$  and the grains in the meander resemble vysotskite  
 307  $(\text{Pd, Fe, Ni})(\text{S, As})$  with low Fe and Ni contents (0–7 wt.% in total).  
 308  
 309 Pt-alloys (n=3 grains) are different from each other in texture, composition and location along  
 310 the stream. One grain close to the quarries is a relict euhedral Pt-Pd-Cu alloy  
 311  $(\text{Pt}_{0.78}\text{Pd}_{0.15}\text{Cu}_{0.07})$ , 20  $\mu\text{m}$  across, that occurs in a composite grain with a broken Pd-  
 312 antimonide (Fig. 9c). The second grain is a 50  $\mu\text{m}$  long tetraferroplatinum  $(\text{Pt}_{1.05}$   
 313  $(\text{Fe, Ni, Cu})_{0.95})$  included in a wrinkled Pd-antimonide from the meander zone (Fig. 9e).  
 314 Another particle of similar composition was also located enclosed by sperrylite in polished  
 315 sections (Fig. 8a). The third grain is a subrounded, single tetraferroplatinum  $(\text{Pt}_{2.7}$   
 316  $(\text{Fe, Cu, Ni})_{1.3})$ , 60  $\mu\text{m}$  across, that contains lower Ni and Cu totaling < 5 wt.%. This last grain  
 317 belongs to sample C10, downstream, after the meander area. Only one analysis of a 5  $\mu\text{m}$   
 318 sized Pt-Pd-Cu-Sb alloy from the source chromitites is available in the bibliography (Prichard  
 319 and Tarkian, 1988) and comparatively, the alluvial Pt-Pd-Cu alloy found is larger and  
 320 contains more Pt and less Pd (Fig. 10a).  
 321  
 322 Laurite (n=2 grains) is rare in the alluvial assemblage. One grain with Pd-antimonide (Fig.  
 323 7e) in the meander is euhedral and has a pure composition of  $\text{RuS}_2$ . The other grain is the  
 324 only PGM recovered from sample site CS (Fig. 2), the furthest from the Cliff quarries. This is  
 325 a subhedral single grain with a composition similar to  $(\text{Ru, Os})(\text{S, As})_2$ , with up to 14wt.% Os.  
 326 The presence of both Os-Ir-bearing laurite and Os-free laurite with inclusions of native Os  
 327 was also noted in the source rocks (Tarkian and Prichard, 1987; Fig. 10b). Much of this Os is

likely to be derived from the alteration of Os-laurite to pure RuS<sub>2</sub> during serpentinization of the ophiolite (Prichard et al., 2017). Both types of laurite remain in the placers.

Other less abundant PGM in the placers include one grain of palladoarsenide (Fig. 7f), and one grain of ruarsite and another of platarsite (Fig. 8b-c) found only in the polished sections of the alluvial PGM.

### *Gold*

Eight Au-bearing grains from 30 to 80 µm in diameter have been identified. Five of these occur as single particles of electrum with up to 25wt.% Ag (Table 3). Only one irregular grain of electrum was recovered close to the Cliff quarries (Fig. 12a). Electrum in the meander zone occurs as subhedral pitted grains (Fig. 12b), round smooth grains (Fig. 12c) and as a porous grain with a delicate structure (Fig. 12d). Gold-bearing phases also occur as thin covers on the surfaces of PGM and Au. For example, pitted electrum is observed on the surface of a Pd-antimonide (Fig. 9d) and pitted Au-(Cu-Pt-Pd) occurs on the surface of a composite grain of hollingworthite and Au (Fig. 11f). Downstream, a Au-Pd cover with up to 2.6 wt.% Pd was observed on a composite grain of Pd-antimonide and sperrylite. Some placer gold particles at Cliff (Fig. 12a-d) mimic the textures of the gold grains located in the source rocks, where rounded and porous particles were detected (Fig. 13a-b).

### *Alluvial PGM at Harold's Grave*

The results from panning at Harold's Grave were less successful and the source rocks here are dominated by IPGM (Table 2). PGM and gold were recovered from samples HG1, 2, 7 and 10 (Table 2), so they are erratically distributed though the sampling sites. One euhedral composite grain of 40 µm laurite (Ru<sub>0.98</sub>S<sub>2.02</sub>) with iridium (Ir-Fe-(S,As)), as well as one 60

μm grain of osmium ( $\text{Os}_{0.9}\text{Ir}_{0.06}\text{Ru}_{0.04}$ ) with subhedral shape and pitted edges were recovered from the panned material.

In addition, four Au grains up to 300x400 μm in size were also recovered. They are all relatively pure in terms of composition. Two grains of Au, both with minor contents of Cu (4–17 wt.%), exhibit the same fine porous texture on their surfaces, although one is euhedral and the other is subrounded. The other two grains (Fig. 12e-f) are subhedral and very porous aggregates. They consist of subrounded particles of Au with minor amounts of Ag in composition (6 wt.% on average) and show formations of pure dendritic Au on their surfaces.

## **Discussion**

Examination of the placer PGM derived from the Shetland PGE-rich chromitites at Cliff and Harold's Grave allows for the comparison between PGM assemblages in the source rocks and streams in order to identify the most relevant modifications of the alluvial minerals and assess their origin.

### ***Evolution of placer PGM from the rocks***

The source rock PGM assemblage is represented by those listed in Tarkian and Prichard (1987) and Prichard and Tarkian (1988), and it is also described in Prichard et al. (1986; 1988; 1994; 2017). Estimation of the percentages of each type of PGM given in Tables 1 and 2, and in Fig. 4a, is illustrative and for comparison purposes only. Prichard et al. (1994) also observed oxidised Pt and Pd phases in the chromite-rich rocks at Cliff. More recently, an extensive study of the PGM was carried out to find Os-bearing minerals for Os isotope analysis (e.g. Prichard et al., 2017). This revealed, in addition to those PGM already described, significant oxidation of the PGM including oxidised Pt-Pd-Ni-Cu-alloys and

sperrylite. One grain of Pd-O, 60 µm in diameter, was also located. There is also the occurrence of breithauptite (NiSb) containing approximately 1% Pd as well as geversite (PtSb<sub>2</sub>), Pt-Fe alloy and one Pd-Te-Sb-Bi (Fig. 13c-f). In the more recent survey it became clear that many of the laurite and clusters of PPGM grains have sizes in the rocks of 30-40 µm, reaching up to 60 µm.

#### *Cliff*

The placer PGM assemblage recovered at Cliff reflects the type and abundance of those PGM in the rocks but there is less variety in the alluvial concentrates (Fig. 4a). Alluvial PGM are equally dominated by sperrylite, Pd-antimonides and sulfarsenides. In addition, Pd-sulfides, Pd-arsenide, platarsite and ruarsite (totalling 8 grains only) were also recovered from the streams. Millerite and nickeline are barren of PGE and occur only as internal inclusions in sperrylite. Scarce Pt-alloys (Pt-Pd-Cu, Pt-Fe) and laurite complete the alluvial PGM assemblage. Electrum and Cu-Pt- and Pd-bearing gold also occur as both single grains and coatings on detrital PGM. Alluvial PGM and associated gold have average sizes of 21 x 76 µm, and range from 5 to 110 µm in diameter.

Compared with the source rocks, there is a clear increase in sperrylite (>24%) and decrease in stibiopalladinite (<10%), irarsite and hollingworthite (<7%), and Pt-alloys (<2%) in the streams. Composite PGM of sperrylite with Pd-antimonide, irarsite and laurite occur in both the source rocks and placers. Laurite is equally scarce in rocks and streams (Fig. 4). The least abundant PGM in the rocks such as native Os, Rh-Sb-S, geversite (PtSb<sub>2</sub>), potarite (PdHg) or rare Pd-Te phases are absent in the streams. Nickel- and Cu-bearing phases in the rocks such as ruthenian pentlandite, hongshiite (PtCu), Ni-Cu alloys, and native Cu, have not been



located in the alluvial concentrates either. Likewise, oxidised Pt- and Pd-phases are absent in the streams.

The composition of the common PGM between rocks and streams is rather similar, although some alluvial PGM such as irarsite, hollingworthite and Pt-alloys exhibit increase Pt contents while alluvial Pd-antimonides show a progressive loss of Pd. Increased Rh content is also observed in alluvial irarsite (Fig. 10a, b). Gold-bearing particles have a similar composition (Au-Pd, Au-Cu-Pt), although electrum dominates the alluvial assemblage.

Placer PGM are mainly concentrated where the stream meanders have formed, from which 58% of the PGM found were recovered (Fig. 4b). Only one grain of laurite was located towards the basal thrust. At this point the slope gradient and the water flow are intense, forming a waterfall under which loose sediment is deposited (Fig. 3e) and where a greater accumulation of heavy minerals is expected. Thus, it is clear that a great part of the alluvial PGM has been concentrated close to the quarries, particularly in the suitable meander zone, but PGM have not been able to travel further downstream.

The types of placer PGM do not vary significantly downstream. The most abundant PGM persist throughout the stream and have similar sizes. However, the shape of the alluvial PGM does vary and the PGM often show signs of disintegration downstream. Sperrylite and Pd-antimonides exhibit these variations most clearly as they are the most common PGM observed. Sperrylite, where it occurs close to the source rocks, retains its euhedral and angular form (Fig. 5) whereas further downstream it shows smoother surfaces and becomes progressively more rounded (Fig. 6). Pd-antimonides, where they are observed close to the quarries, are subhedral and have silicates attached to their surfaces whereas in the meander

zone, these silicates are absent and the PGM may show lamellar structures. Further downstream, etching of Pd-antimonides is common in the form of concave faces or irregular surfaces (Fig. 9). The same is observed for Pd-sulfides, which are euhedral close to the quarries but appear broken down in the meander zone. Also for Pt-alloys, which are enclosed by other PGM close to the source rocks but appear as single, subrounded Pt-Fe particles downstream.

#### *Harold's Grave*

At Harold's Grave, PGM are dominated by IPGM (Tarkian and Prichard 1987; Prichard et al., 1988, 2017). The IPGM assemblage in the rocks (Table 2) consists of laurite, osmium, irarsite and IrSbS. The size of the IPGM in the rocks ranges from a few microns to 500  $\mu\text{m}$ , as found by Badanina et al. (2013, 2016) from concentrates of the rocks produced using the hydroseparation technique, and by Prichard et al. (2017) using 3D X-ray tomography. The PPGM are hollingworthite and scarce hongshiite (PtCu), Pt-alloy (Pt-Pd-Cu), genkinite and Pd-, Rh- and Ni-bearing antimonides totalling 9 grains only (<10%; Table 2). The survey by Prichard et al. (2017) corroborates that PPGM, including minor sperrylite, Pt-Fe alloys and platarsite, typically occur in clusters with Ru-pentlandite and some IPGM interstitially to chromite grains.

The placer PGM located at Harold's Grave (n=3 grains) consist of laurite, iridium alloy and osmium alloy, with sizes ranging from 20 to 60  $\mu\text{m}$ . No PPGM or pentlandite were recovered (Table 2). Despite the scarce PGM recovered, these represent the most abundant PGM in the IPGE-rich chromitites at Harold's Grave. The presence of gold is noteworthy. Detrital grains of Au-Cu have been detected but electrum and native Au also occur in porous aggregates up to 400  $\mu\text{m}$  across with dendritic growths of native Au on surface. The sizes of the alluvial

PGM and Au at Harold's Grave are in the range of those in the source rocks. No other statistically significant conclusions can be drawn due the low recovery of placer PGM in the panned samples.

#### *Modification of PGM and PGE mobility*

Overall, only slight differences are observed between the PGM assemblages of the rocks and streams:

(i) Those PGM enclosed by or in the edges of chromite grains in the source rocks are poorly represented or absent in the streams, suggesting that they may remain protected by their host minerals in the alluvial sands. This is mainly the case for Ru- and Os-PGM (laurite, osmium) within chromite grains in the rocks. Potarite (PdHg) also occurs in chromite, and antimonides (RhSbS, IrSbS, Rh-Ni-Sb, NiSb, Pd-Cu-Sb and genkinite) are often located in clusters within irarsite (Tarkian and Prichard, 1987; Prichard and Tarkian, 1988). The lack of these PGM in the streams is more evident at Harold's Grave, where the source chromitites are IPGE-enriched. In this case, however, the small dense fraction recovered may reflect lower erosion and a more restricted liberation of the host minerals and PGM into the streams.

(ii) PGM that occur in the silicate matrix interstitial to chromite grains in the rocks, less protected against weathering, are largely represented in the streams at Cliff. These are sperrylite, stibiopalladinite, irarsite–hollingworthite–platarsite and Pt-alloys. Of these, sperrylite is the most resistant whereas Pd-, Ir- and Rh-PGM decrease in number and show slight changes in their composition (Figs. 4, 10). Their abundance and composition suggest some progressive Pd-loss and Pt-gain in the streams. For example, alluvial stibiopalladinite grains extend towards Pd<sub>5</sub>Sb<sub>3</sub> compositions and show a loss of up to 14wt.% Pd. The alluvial Pt-Pd-Cu alloy contains less Pd (< 8 wt.%) and more Pt (>25 wt.%) than its counterpart in the

477 rocks, and isoferroplatinum ( $\text{Pt}_3\text{Fe}$ ) only occurs in the streams. Irarsite and hollingworthite  
 478 also contain more Pt ( $>4\%$ ) in the streams than in the rocks (Fig. 10b).

479

480 (iii) There are some losses of PGE-bearing phases from the rock assemblage into the streams.  
 481 The most notable of these is the loss of all Pt and Pd oxides, which are poorly resistant  
 482 compounds typically on the edges of broken PGM (Fig. 13d-e) that are not preserved during  
 483 the transportation process. The disappearance of PGE-oxides or -hydroxides from source  
 484 rocks in the fluvial environment has been previously reported from rivers draining the Great  
 485 Dyke in Zimbabwe (Oberthür et al., 2003, 2013) and the Freetown layered complex in Sierra  
 486 Leone (Bowles et al., 2017a, 2017b). Bowles et al. (2017b) also noted the low stability of Cu-  
 487 bearing sulfides and PGM such as tulameenite ( $\text{Pt}_2\text{FeCu}$ ) during weathering of the rocks.

488

489 The low stability of Cu- and also Ni-bearing phases is also inferred from the eroded  
 490 chromitites at the Shetland complex, as most of them (e.g. Ru-pentlandite, hongshiite  $\text{PtCu}$ ,  
 491 and Cu-bearing alloys) are largely absent in the streams. All these phases occur in interstitial  
 492 positions to chromite grains in the rocks. For example, hongshiite occurs at the edge of  
 493 sperrylite and intergrown with Ni-Cu alloys, while Pt-Pd-Au-Cu and Pd-Cu alloys occur in  
 494 composite grains with native Cu (Tarkian and Prichard, 1987; Prichard and Tarkian, 1988).  
 495 Of all these, only sperrylite and one Pt-Pd-Cu alloy in stibiopalladinite remain in the streams.  
 496 It is worth noting that Cu-bearing phases are scarce in the source rocks (Table 2) and some of  
 497 them could have been missed during preparation of the panned samples. However, Ni- and  
 498 Cu-intermetallic compounds and sulfides, and moreover pentlandite, are highly unstable  
 499 phases in supergene conditions, and Ni and Cu can be lixiviated in a wide range of oxidizing  
 500 Eh and acid to neutral pH conditions (Garrels and Christ, 1965; Williams, 1990; Takeno,

2005). Thus, Cu-bearing PGM from the Shetlands chromitites, if not protected by their host (e.g. Fig. 8a, d; Fig. 9e), may have been destroyed during weathering.

(iv) The textures and composition of the gold grains (Au-Pd, Au-Cu) in the rocks almost exactly mimic those in the placers with both rounded grains and spongy textured grains observed (Fig. 13a-b). They are clearly an integral part of the precious metal occurrence at Cliff as they are located in the rocks and have not been derived from carriage by say boulder clay from outside the area. Only dendritic growths of pure Au over Au-(Ag) grains at Harold's Grave may reflect some remobilization of Au at the grain scale (Fig. 12e-f). These particles satisfy the model for secondary Au formation described in Hough et al. (2011), which integrates a primary origin of the Au grains with secondary mobilization and aggregation processes on grains surfaces. This secondary Au typically displays high purity, very fine crystallinity, and a wide variety of morphologies, resulting from Au/Ag dissolution and Au precipitation acting simultaneously on the surface of the grains.

Although it is difficult to evaluate the metal mobility based on mineralogical observations alone, these data suggest that there is a preferential mobility of Pd, Cu, Ni and some Au over other metals (i.e. Pt, Rh, Ir, Os, Ru) in the secondary environment of the Shetland ophiolite complex.

### ***Origin of the PGM***

The overall similarity of the PGM assemblages of the PGE-rich rocks and the associated streams suggests that the PGM have weathered from the rock and their short transport distances have allowed them to preserve largely their compositions and often euhedral shapes. There are some losses from the rock assemblage, but the PGM assemblage in the

rocks is very similar to that in the streams. The PGM in the streams are of a similar size to the larger PGM in the rocks reflecting a mechanical transportation process rather than a growth in situ of the PGM. This suggests early stages of dispersal of the PGE from the quarries.

The long standing debate concerning the mechanical erosion of PGM from the source rocks versus the growth of PGM in situ downstream of the source has been a point of controversy for years. The sometimes contrasting mineralogical assemblages and PGM composition between sources and placers, the delicate morphologies and larger size of placer nuggets compared to primary PGM in the rocks or their isotopic signatures, all have been used in discussion to support both models.

It is considered that placer PGM are normally primary and are mechanically eroded from the source rocks (e.g. Cabri et al., 1996; Weiser, 2002; and references therein). In some complexes they may indeed be large PGM that are simply eroded from the rocks, as for example in some Ural-Alaskan type complexes. Some large PGM have been located in lode placers from the Nizhni Tagil and Kachkanar dunite massifs in the Uranium Platinum Belt, in the Vetraya-Vyvenka Belt of Kamchatka, Russian Far East, or in the dunite core of the Pt-rich Alto Condoto Complex in Colombia (Weiser, 2002 and references therein). Rare, large PGM also occur in the oxidized Main Sulfide Zone of the Great Dyke, Zimbabwe (Oberthür et al., 2003) and also in the Shetland chromitites (Badanina et al., 2013).

Doubt was cast when Ottemann and Augustithis (1967) proposed that polyphase Pt-Fe nuggets in a laterite capping the massif of Yubdo (Ethiopia) formed at low temperatures by 'element agglutination'. Later, it was proposed that weathering of the rocks aided by organic acids in the soils alter and break down primary PGM liberating the PGE, which can be

transported in solution through the soils down slope. Soils close to rivers or stream banks where Eh and pH conditions change allow for the precipitation of the PGE and the growth of PGM (Bowles, 1986; 1988; Bowles et al., 1994a, 1994b, 1995). Selective metal leaching during weathering to form supergene PGM has been documented for the perfectly crystallized eluvial and alluvial PGM from the Freetown Igneous Complex, Sierra Leone (e.g. Bowles 1995; Bowles et al., 2013, 2017a, 2017b). Also for the oxidized Main Sulfide Zone of the Great Dyke, Zimbabwe and associated Pt-dominated alluvials (Oberthür et al., 2003), as well as for the botryoidal and arborescent Pt-Pd aggregates and the Pt-enriched rims on detrital PGE-alloys from the Bom Succeso stream in Minas Gerais, Brazil (Cabral et al., 2007, 2009).

There are many other examples of PGE-bearing phases that apparently formed in low temperature conditions (~100–25°C) in varied deposits. One example are the internally zoned Au-Pd arborescent grains from Hope's Nose, UK (Leake et al., 1991) and Serra do Espinhaço, Minas Gerais (Cabral et al., 2008). Another example are the rosettes of native Pd on the surface of gold nuggets from Gongo Soco Fe-ores, Minas Gerais (Cabral and Kwitko-Ribeiro, 2004) and the Pd-Cu rosettes coating goethite in the Limoeiro Ni-Cu-(PGE) deposit (Mota-e-Silva et al., 2016). Neoformed Pt-Ir-Fe-Ni alloys and layers of Ir-rich alloys on multistage PGE-grains are reported from Ni-laterites in the Falcondo mining area (Dominican Republic, Aiglsperger et al., 2016). It appears that supergene precipitation of PGE could be aided by both biogenic activity (Reith et al., 2016; Bowles et al., 2017b) and inorganic processes such as bioreduction or electrochemical accretion of metals (e.g. Cabral et al., 2011; Aiglsperger et al., 2016).

The resolution to this controversy may be partially explained in that both ideas are correct in certain circumstances. Mechanical erosion may be more prominent in high latitudes where mechanical erosion dominates over chemical weathering. However, in tropical conditions, chemical weathering dominates and PGM may precipitate in situ, perhaps in soils or stream banks distally to the source rocks following the chemical disintegration of the primary PGM. Rock-weathering conditions in humid and temperate zones, with high rainfall and abundant organic material would enhance PGE mobility and redeposition. It is clear that both primary (magmatic or hydrothermally modified) PGM mechanically liberated from the rocks and secondary, reworked or neoformed supergene PGE-bearing minerals, can coexist in some eluvial and alluvial placers.

In the Shetland Islands mechanical erosion dominates and is operating only on a small scale very close to the source. The PGM in the streams reflect the source rocks as they are very close to them. There are signs of disintegration of the PGM as they travel downstream. Pd-antimonides weather to produce furrowed surfaces and concave etched surfaces whereas sperrylite starts with jagged edges that become rounded downstream. The greater initial disintegration of Pd-bearing phases over sperrylite observed at Cliff may be a result of the greater mobility of Pd over Pt which has been consistently observed, including in surficial weathering environments (e.g. Fuchs and Rose, 1974; Wood and Vlassopoulos, 1990; Prichard and Lord, 1994; Salpéteur et al., 1995; Prichard et al., 2001; Suárez et al. 2010, Bowles et al., 2013). Sperrylite is harder than Pd-antimonides and has proved to be considerably more durable and resistant to weathering and mechanical erosion (e.g., Oberthür et al., 2003, 2013; Suárez et al., 2010), which also appears true in this study of placer PGM at the Shetlands ophiolites.



## 600   **Conclusions**

601   The PGM assemblage in the streams at Cliff consists dominantly of sperrylite and Pd-  
602   antimonides and this is reflected by the PGM found in the rocks. The extreme proximity of  
603   the source to the streams and the well documented PGM assemblage in the rocks allows a  
604   comparison of PGM compositions and sizes in the rocks against those in the streams. This  
605   reveals that the assemblages are very similar although there are notable absences of some  
606   PGM types in the streams. The Pt and Pd oxides in the rocks are missing in the streams,  
607   demonstrating that they are very fragile and unlikely to survive erosion. Ni-sulfides and Cu-  
608   bearing PGM and alloys are also unstable phases that remain in the streams only when  
609   protected by their original host minerals. Thus there is a continuum from magmatic formation  
610   and hydrothermal upgrading of the PGM assemblage in the rocks through to initial  
611   weathering and oxidation of the PGM in the rocks through to erosion into the streams. Within  
612   the streams there is further evidence of change in the PGM assemblage. More resistant  
613   minerals such as sperrylite persist downstream becoming more rounded whereas Pd  
614   antimonides can be observed in the early stages of disintegration with concave etching on  
615   their surfaces. Laurite and members of the irarsite–hollingworthite–platarsite solid solution  
616   series are also preserved in the streams. The common Pt-Fe alloys observed in many placer  
617   deposits are largely absent. The gold grains in the streams are eroded from the Cliff  
618   assemblage in the rocks as indicated by the close similarity of the textures that they show in  
619   both the rocks and in the streams. The presence of Au-Pd and Au-Cu layers over primary  
620   PGM and of native Au in dendritic growths may indicate a local remobilization of these  
621   elements in surface conditions, at least on the grain scale. Otherwise the PGM assemblage  
622   preserved in the streams at Cliff is early stage with PGM having been mechanically eroded  
623   from the nearby source rocks and there is no evidence of growth in situ of PGM in the placers  
624   rather mechanical disintegration. This is early stage mechanical erosion and so the usual Os-

Ir-Ru alloys that characterises ophiolitic placer PGM are not present. This is more evident at Harold's Grave, where the few IPGM found in the streams reflect the restricted release of the PGM enclosed by primary minerals in the source rocks. In general, the alluvial PGM assemblage found in the streams draining the Shetland complex mimics the rather unusual suite of PGM in the PGE-rich ophiolitic rocks.

## Acknowledgements

We would like to thank The Department of Education, Universities and Research of the Basque Government (Refs. IT762-13, BFI-2011-254) for additional funding and Dr. R.S. Garcia (UPV/EHU) for her technical support. We also thank the helpful comments by Dr. F. Zaccarini and another anonymous referee, which greatly improved the quality of the manuscript, and Drs. I. McDonald and B. O'Driscoll for the editorial handling. The coauthors of this work are very grateful to D.R. Sharp, A. Colling and Dr. J.F.W. Bowles for their contributions to this manuscript. We dedicate this work with all of our love to Prof. Hazel M. Prichard and John S. Watson.

## References

- Aiglsperger, T., Proenza, J.A., Font-Bardia, M., Baurier-Aymat, S., Galí, S., Lewis, J.F. and Longo, F. (2016). Supergene neoformation of Pt-Ir-Fe-Ni alloys: multistage grains explain nugget formation in laterites. *Mineralium Deposita*, Published on-line 12 November 2016, <https://doi.org/10.1007/s00126-016-0692-6>.
- Augé, T., Legendre, O. and Maurizot, P. (1998) The distribution of Pt and Ru-Os-Ir minerals in the New Caledonia ophiolite. Pp. 141–154 in: International Platinum (P.N. Laverov and V. V. Distler, editors). Theophrastus publications, St. Petersburg, Athens.

649 Bacuta, G. C. J., Lipin, B. R., Gibbs, A. K. and Kay R.W. (1988) Platinum-group element  
650 abundance in chromite deposits of the Acoje ophiolite block, Zambales ophiolite  
651 complex, Philippines. Pp. 381–382 in: Geo-Platinum Symposium Volume (H. M.  
652 Prichard, P. J. Potts, J. F. W. Bowles and S. J. Cribb, editors). Elsevier.

653 Badanina, I. Y., Malitch, K. N., Lord, R. A. and Meisel, T. C. (2013) Origin of primary  
654 assemblage in chromitite from a mantle tectonite at Harold's Grave (Shetlan Ophiolite  
655 Complex, Scotland). *Mineralogy and Petrology*, **107**, 963–970.

656 Badanina I. Y., Malitch K. N., Lord R. A., Belousova E. A. and Meisel T. C. (2016) Closed-  
657 system behaviour of the Re–Os isotope system recorded in primary and secondary  
658 platinum-group mineral assemblages: evidence from a mantle chromitite at Harold's  
659 Grave (Shetland Ophiolite Complex, Scotland). *Ore Geology Reviews*, **75**, 174–185.

660 Bowles, J. F. W. (1986) The development of platinum-group minerals in laterites. *Economic*  
661 *Geology*, **81**, 1278–1285.

662 Bowles, J.F.W. (1988) Further studies of the development of platinum-group minerals in the  
663 laterites of the Freetown Layered Complex, Sierra Leone. Pp. 273–280 in: Proceedings  
664 of the symposium Geo-Platinum 87. (H.M. Prichard, P.J. Potts, J.F.W. Bowles and S.J.  
665 Cribb, editors). Elsevier Applied Science, London.

666 Bowles, J. F. W. (1995) The development of platinum-group minerals (PGM) in laterites:  
667 mineral morphology. *Chronique de la Recherche Minière*, **520**, 55–63.

668 Bowles, J.F.W., Gize, A.P. and Cowden, A. (1994a) The mobility of the platinum-group  
669 elements in the soils of the Freetown Peninsula, Sierra Leone. *The Canadian*  
670 *Mineralogist*, **32**, 957–967.

671 Bowles, J.F.W., Gize, A.P., Vaughan, D.J. and Norris, S.J. (1994b) The development of  
672 platinum-group minerals in laterites; an initial comparison of the organic and inorganic

673 controls. *Transactions of the Institute of Mining and Metallurgy, B Applied Earth*  
674 *Science*, **103**, 53–56.

675 Bowles, J.F.W., Gize, A.P., Vaughan, D.J. and Norris, S.J. (1995) Organic controls on  
676 platinum-group element (PGE) solubility in soils: initial data. *Chronique de la Recherche*  
677 *Minière*, **520**, 65–73.

678 Bowles, J.F.W., Lyon, I.C., Saxton, J.M. and Vaughan, D.J. (2000) The origin of platinum  
679 group minerals from the Freetown Intrusion, Sierra Leone, inferred from osmium isotope  
680 systematics. *Economic Geology*, **95**, 539–548.

681 Bowles, J.F.W., Prichard, H. M., Suárez, S. and Fisher, P.C. (2013) The first report of  
682 platinum-group minerals in magnetite-bearing gabbro, Freetown layered Complex, Sierra  
683 Leone: occurrences and genesis. *The Canadian Mineralogist*, **51**, 455–473.

684 Bowles, J.F.W., Suárez, S., Prichard, H. M. and Fisher, P.C. (2017a) Weathering of PGE  
685 sulfides and Pt–Fe alloys in the Freetown Layered Complex, Sierra Leona. *Mineralium*  
686 *Deposita*. Published on-line 20 January 2017, [https://doi.org/10.1007/s00126-016-](https://doi.org/10.1007/s00126-016-0706-4)  
687 [0706-4](https://doi.org/10.1007/s00126-016-0706-4).

688 Bowles, J.F.W., Suárez, S., Prichard, H. M. and Fisher, P.C. (2017b) The mineralogy,  
689 geochemistry and genesis of the alluvial platinum-group minerals of the Freetown  
690 Layered Complex, Sierra Leone. *Mineralogical Magazine*. Published on-line 19 June  
691 2017, <https://doi.org/10.1180/minmag.2017.081.032>.

692 Bridges, J. C., Prichard, H. M., Neary, C. R. and Meireles, C. A. (1993) Platinum-group  
693 element mineralization in the chromite-rich rocks of the Braganca massif, northern  
694 Portugal. *Transactions Institute Mining Metallurgy, B Applied Earth Science*, **102**,  
695 103–113.

696 Brough, C. P., Prichard, H. M., Neary, C. R., Fisher P. C. and McDonald, I. (2015)  
697 Geochemical variations within podiform chromitite deposits in the Shetland Ophiolite:

698 Implications for petrogenesis and PGE concentration. *Economic Geology*, **110**, 187–  
699 208.

700 Cabral, A.R. and Kwitko-Ribeiro, R. (2004) On the rosettes of "native palladium" from  
701 Minas Gerais, Brazil: evidence from Gongo Soco. *The Canadian Mineralogist*, **42**,  
702 683–674.

703 Cabral, A.R., Beaudoin, G., Choquette, M., Lehmann, B. and Polônia, J.C. (2007) Supergene  
704 leaching and formation of platinum in alluvium: evidence from Serro, Minas Gerais,  
705 Brazil. *Mineralogy and Petrology*, **90**, 141–150.

706 Cabral, A.R., Tupinambá, M., Lehmann, B., Kwitko-Ribeiro, R. and Vymazalová, A. (2008)  
707 Arborescent palladiniferous gold and empirical Au<sub>2</sub>Pd and Au<sub>3</sub>Pd in alluvium from  
708 southern Serra do Espinhaço, Brazil. *Neues Jahrbuch für Mineralogie Abhandlungen*,  
709 **148/3**, 329–336.

710 Cabral, A. R., Lehmann, B., Tupinambá, M., Schlosser, S., Kwitko-Ribeiro, R. and Abreu, F.  
711 R. (2009) The platiniferous Au-Pd belt of Minas Gerais, Brazil, and genesis of its  
712 botroidal Pt-Pd aggregates. *Economic Geology*, **104**, 1265–1276.

713 Cabral, A. R., Radtke, M., Munnik, F., Lehmann, B., Reinholz, U., Riesemeier, H.,  
714 Tupinambá, M. and Kwitko-Ribeiro, R. (2011) Iodine in alluvial platinum–palladium  
715 nuggets: Evidence for biogenic precious-metal fixation. *Chemical Geology*, **281**, 125–  
716 132.

717 Cabri, L. J. and Harris, D. C. (1975) Zoning of Os-Ir alloys and the relation of the geological  
718 and tectonic environment of the source rocks to the bulk Pt:Pt+Ir+Os ratio for placers.  
719 *The Canadian Mineralogist*, **13**, 266–274.

720 Cabri, L. J., Harris, D. C. and Weiser, T. W. (1996) Mineralogy and petrology of platinum-  
721 group mineral (PGM) placer deposits of the world. *Exploration and Mining Geology*, **5**,  
722 73–176.

- 723 Corrivaux, L. and Laflamme, J. H. G. (1990) Minéralogie des éléments du groupe du platine  
724 dans les chromitites de l'ophiolite de Thetford mines, Québec. *The Canadian*  
725 *Mineralogist*, **28**, 579–595.
- 726 Derbyshire, E.J., O'Driscoll, B., Lenaz, R., Gertisser, R. and Kronz, A. (2012)  
727 Compositionally heterogeneous podiform chromitite in the Shetland Ophiolite Complex  
728 (Scotland): Implications for chromitite petrogenesis and late stage alteration in the  
729 upper mantle portion of a supra-subduction zone ophiolite. *Lithos*, **162-163**, 279–300.
- 730 Escayola M., Garuti D., Zaccarini F., Proenza J., Bédard J.H. and Van Staal, C. (2011)  
731 Chromitite and Platinum-Group-Element Mineralization at Middle Arm Brook, Central  
732 Advocate Ophiolite Complex, Baie Verte Peninsula, Newfoundland, Canada. *The*  
733 *Canadian Mineralogist*, **49**, 1523–1547.
- 734 Flinn, D. (1985) The Caledonides of Shetland. Pp. 1159–1172 in: The Caledonide Orogeny  
735 - Scandinavia and related Areas (D. G. Gee and B. A. Sturt, editors.). John Wiley and  
736 Sons Ltd.
- 737 Fuchs, W.A. and Rose, A.W. (1974) The Geochemical Behavior of Platinum and Palladium  
738 in the Weathering Cycle in the Stillwater Complex, Montana. *Economic Geology*, **69**,  
739 332–346.
- 740 Garrels, R.M. and Christ, C.L. (1965) Solutions, minerals, and equilibria. Harper & Row,  
741 Publishers, New York, 450 p.
- 742 González-Jiménez, J.M., Griffin, W.L., Proenza, J.A., Gervilla, F., O'Reilly, S.Y., Akbulut,  
743 M., Pearson, N.J. and Arai, S. (2014). Chromitites in ophiolites: How, where, when,  
744 why? Part II. The crystallization of chromitites. *Lithos*, **189**, 140–158.
- 745 Grammatikopoulos, T.A., Kapsiotis, A., Zaccarini, F., Tsikouras, B., Hatzipanagiotou, K. and  
746 Garuti, G. (2007). Investigation of platinum-group minerals (PGM) from Pindos

747 chromitites (Greece) using hydroseparation concentrates. *Minerals Engineering*, **20**,  
748 1170–1178.

749 Hough, R., Noble, R. and Reich, M. (2011) Natural gold nanoparticles. *Ore Geology Review*,  
750 **42**, 55–61.

751 Kim, W.-S. and Chao G. Y. (1991) Phase relations in the system Pd-Sb-Te. *The Canadian*  
752 *Mineralogist*, **29**, 401–409.

753 Kozlu, H., Prichard, H. M., Melcher, F., Fisher, P. C., Brough, C. and Stueben D. (2014)  
754 Platinum group element (PGE) mineralisation and chromite geochemistry in the Berit  
755 ophiolite (Elbistan/Kahramanmaraş), SE Turkey. *Ore Geology Reviews*, **60**, 97–111.

756 Leake, R. C., Bland, D. J., Styles, M. T. and Cameron, D. G. (1991) Internal structure  
757 of Au-Pd-Pt grains from south Devon, England in relation to low temperature  
758 transport and deposition. *Transactions of the Institute of Mining and Metallurgy*,  
759 *B Applied Earth Science*, **100**, B159–178.

760 Lord, R. A., Prichard, H. M. and Neary, C. R. (1994) Magmatic PGE concentrations  
761 and hydrothermal upgrading in the Shetland ophiolite complex. *Transactions*  
762 *Institute Mining Metallurgy, B Applied Earth Science*, **103**, B87–162.

763 Moreno, T., Prichard, H., Lunar, R., Monterrubio, S. and Fisher, P. (1999). Formation  
764 of a secondary platinum-group minerals assemblage in chromitites from the  
765 Herbeira ultramafic massif in Cabo Ortegal, NW Spain. *European Journal of*  
766 *Mineralogy*, **11**, 363–378.

767 Moreno, T., Gibbons, W., Prichard, H.M. and Lunar, R. (2001). Platiniferous  
768 chromitite and the tectonic setting of ultramafic rocks in Cabo Ortegal, NW  
769 Spain. *Journal of the Geological Society*, **158**, 601–614.

770 Mota-e-Silva, J., Prichard, H.M., Suárez, S., Ferreira Filho, C.F. and Fisher, P.C.  
771 (2016) Supergene alteration of platinum-group minerals and the formation of Pd-

772 Cu-O and Pd-I-O compounds in the Limoeiro Ni-Cu-(PGE) deposit, Brazil. *The*  
773 *Canadian Mineralogist*, **54**, 755–778.

774 Oberthür, T., Weiser, T.W. and Gast, L. (2003) Geochemistry and mineralogy of platinum-  
775 group elements at Hartley Platinum Mine, Zimbabwe Part 2. Supergene redistribution  
776 in the oxidized Main Sulfide Zone of the Great Dyke, and alluvial platinum group  
777 minerals. *Mineralium Deposita*, **38**, 344–355.

778 Oberthür, T., Weiser, T.W., Melcher F., Gast, L. and Wöhr, C. (2013) Detrital platinum-  
779 group minerals in rivers draining The Great Dyke, Zimbabwe. *The Canadian*  
780 *Mineralogist*, 51, 197–222.

781 Ohnenstetter, M., Johan, Z., Coherie, A., Fouillac, A., Guerrot, C., Ohnenstetter, D.,  
782 Chaussidon, M., Rouer, O., Makovicky, E., Makovicky, M., Rose-Hansen, J., Karup-  
783 Moller, S., Vaughan, D., Tumer, G., Pattrick, R. A. D., Gize, A.P., Lyon, I. and  
784 McDonald I. (1999) New exploration methods for platinum and rhodium deposits poor  
785 in base-metal sulfides. *Transactions Institute Mining Metallurgy, B Applied Earth*  
786 *Science*, **108**, 119–150.

787 Orberger, B., Fredrich, G. and Woermann, E. (1988) Platinum-group element mineralisation  
788 in the ultramafic sequence of the Acoje ophiolite block, Zambales, Philippines. Pp  
789 391–380 in: Geo-Platinum Symposium Volume (H. M. Prichard, P. J. Potts, J. F. W.  
790 Bowles, S. J. Cribb, editors). Elsevier.

791 O'Driscoll, B. and González-Jiménez, J.M. (2016) Petrogenesis of the Platinum-Group  
792 Minerals. *Reviews in Mineralogy & Geochemistry*, **81**, 489–578.

793 Ottemann, J. and Augustithis, S.S. (1967) Geochemistry and Origin of "Platinum-Nuggets" in  
794 Lateritic Covers from Ultrabasic Rocks and Birbirites of W. Ethiopia. *Mineralium*  
795 *Deposita*, **1**, 269–277.



796 Pedersen, R.B., Johannesen, G.M. and Boyd, R. (1993) Stratiform PGE mineralisations in the  
 797 ultramafic cumulates of the Leka ophiolite complex, central Norway. *Economic*  
 798 *Geology*, **88**, 782–803.

799 Prichard, H. M. (1985) The Shetland Ophiolite. Pp 1173–1184 in: The Caledonide Orogeny -  
 800 Scandinavia and related Areas (D. G. Gee and B. A. Sturt, editors.). John Wiley and  
 801 Sons Ltd.

802 Prichard, H. M. and Brough, C.P. (2009) Potential of ophiolite complexes to host PGE  
 803 deposits. Pp. 277–290 in: New Developments in magmatic Ni-Cu and PGE deposits (C.  
 804 Li and E. M. Ripley, editors.). Geological Publishing House, Beijing.

805 Prichard, H. M. and Lord, R.A. (1993) An overview of the PGE concentrations in the  
 806 Shetland ophiolite complex. Pp. 273–294 in: Magmatic Processes and Plate Tectonics  
 807 (H. M. Prichard, T. Alabaster, N. B. Harris, C. R. Neary, editors). Volume **76**,  
 808 Geological Society of London.

809 Prichard, H.M. and Lord, R.A. (1994) Evidence for the mobility of PGE in the secondary  
 810 environment in the Shetland ophiolite complex. *Transactions Institute Mining*  
 811 *Metallurgy, B Applied Earth Science*, **103**, 79–86.

812 Prichard, H. M. and Tarkian M. (1988) Platinum and palladium minerals from two PGE-rich  
 813 localities in the Shetland Ophiolite Complex. *The Canadian Mineralogist*, **26**, 979–990.

814 Prichard, H. M., Neary, C. R. and Potts P.J. (1986) Platinum-group minerals in the Shetland  
 815 Ophiolite. Pp. 395–414 in: Metallogeny of the Basic and Ultrabasic Rocks ( M. J.  
 816 Gallagher, R. A. Ixer, C. R. Neary and H. M. Prichard, editors). Transactions Institute  
 817 Mining Metallurgy.

818 Prichard, H. M., Potts P. J., Neary C. R., Lord R. A. and Ward G. R. (1988) Development of  
 819 techniques for the determination of the platinum-group elements in ultramafic rock

820 complexes of potential economic significance: mineralogical studies. Commission of  
 821 the European Communities. Report EUR 11631, 163 pp. ISBN 92-825-9245-6.

822 Prichard, H. M., Ixer, R. A., Lord, R. A., Maynard, J. and Williams N. (1994) Assemblages  
 823 of platinum-group minerals and sulfides in silicate lithologies and chromite-rich rocks  
 824 within the Shetland Ophiolite. *The Canadian Mineralogist*, **32**, 271–294.

825 Prichard, H.M., Sá, J.H.S. and Fisher, P.C. (2001) Platinum-group mineral assemblages and  
 826 chromite composition in the altered and deformed Bacuri complex, Amapá, North  
 827 Eastern Brazil. *The Canadian Mineralogist*, **39**, 377–396.

828 Prichard, H. M., Economou-Eliopoulos, M. and Fisher, P. C. (2008a) Platinum-group  
 829 minerals in podiform chromitite in the Pindos ophiolite complex, Greece. *The*  
 830 *Canadian Mineralogist*, **46**, 329–341.

831 Prichard, H. M., Neary, C. R., Fisher, P. C. and O'Hara, M. J. (2008b) PGE-rich podiform  
 832 chromitites in the Al'Ays Ophiolite complex, Saudi Arabia: An example of critical  
 833 mantle melting to extract and concentrate PGE. *Economic Geology*, **103**, 1507–1529.

834 Prichard, H. M., Barnes, S. J., Dale, C. W., Godel, B., Fisher, P.C. and Nowell, G. M. (2017)  
 835 Paragenesis of multiple platinum-group mineral populations in Shetland ophiolite  
 836 chromitite: 3D X-ray tomography and in situ Os isotopes. *Geochimica et*  
 837 *Cosmochimica Acta*. Published on-line 4 April 2017,  
 838 <https://doi.org/10.1016/j.gca.2017.03.035>.

839 Reith, F., Zammit, C.M., Shar, S.S., Etschmann, B., Bottrill, R., Southam, G., Ta, C.,  
 840 Kilburn, M., Oberthür, T., Bail, A.S. and Brugger, J (2016) Biological role in the  
 841 transformation of platinumgroup mineral grains. *Nature Geoscience*, **9**, 294–298.

842 Salpéteur, I., Martel-Jantin, B. and Rakotomanana, D. (1995) Pt and Pd mobility in ferrallitic  
 843 soils of the West Andriamena area (Madagascar). Evidence of a supergene origin of  
 844 some Pt and Pd minerals. *Chronique de la Recherche Minière*, **520**, 27–45.

- Suárez, S., Prichard, H. M., Velasco, F., Fisher, P. C. and McDonald, I. (2010) Alteration of platinum-group minerals and dispersion of platinum-group elements during progressive weathering of the Aguablanca Ni-Cu deposit (SW Spain). *Mineralium Deposita*, **45**, 331–350.
- Takeno, N. (2005) Atlas of Eh-pH diagrams. Intercomparison of thermodynamic databases. Geological Survey of Japan Open File Report No.419, 287 p.
- Tarkian, M. and Prichard, H. M. (1987) Irarsite-Hollingworthite Solid-Solution Series and Other Associated Ru-, Os-, Ir-, and Rh bearing PGM's from the Shetland Ophiolite Complex. *Mineralium Deposita*, **22**, 178–184.
- Weiser, T. W. (2002) Platinum-group minerals (PGM) in placer deposits. Pp. 721–756 in: The geology, geochemistry, mineralogy and mineral beneficiation of platinum-group elements. ( L. J. Cabri, editor). Canadian Institute of Mining, Metallurgy and Petroleum, special volume **54**.
- Williams, P.A. (1990) Oxide Zone Geochemistry. Ellis Horwood Series in Inorganic Chemistry, 286 p.
- Wood, S.A. and Vlassopoulos, D. (1990) The dispersion of Pt, Pd, and Au in surficial media about two PGE-Cu-Ni prospects in Quebec. *The Canadian Mineralogist*, **28**, 649–663.
- Zaccarini, F., Pushkarev, E., Garuti, G., Krause, J., Dvornik, G.P., Stanley, C. and Bindi, L. (2013) Platinum group minerals (PGM) nuggets from alluvial-eluvial placer deposits in the concentrically zoned mafic-ultramafic Uktus complex (Central Urals, Russia). *European Journal of Mineralogy*, **25**, 519–531.

## Figure Captions

Figure 1. Geological map showing the locations of the Cliff and Harold's Grave podiform chromitites in the Shetland ophiolite complex.

Figure 2. Geological map of inset in Fig.1 showing the Cliff chromitites and associated streams in detail. Sampling sites C2-12 and CS are labelled.

Figure 3. Sampling sites at Cliff. (a) General view looking west from the disused chromitite pits showing all sampling sites. (b) View of the pond at the pit and of sample site C2. (c) Sample site C5. (d) View of the stream meanders and sample sites C6 to C9. (e) Sample site CS where the streams amalgamate and plunge over the basal thrust of the ophiolite; the site nearest to the Loch of Cliff.

Figure 4. (a) Pie diagrams showing the different PGM located in the chromite-rich rocks from Cliff (illustrative data, from Prichard et al. 1986 and Prichard & Tarkian 1988), and in the streams panned in this study. (b) Bar graphs showing the number of alluvial PGM recovered with increasing distance from the Cliff quarries: pond exit zone (samples C3-C5), following meander zone (samples C6-C9), exit of the meander downstream (samples C10-11) and basal thrust (sample CS). See Table 1 for more detail.

Figure 5. Back-scattered electron images of sperrylites recovered near the disused quarries from samples C3 to C5. Note the frequent cracks and jagged appearance.

Figure 6. Back-scattered electron images of sperrylites from further downstream to the disused quarries from samples C6 to C11. Note more rounded appearance than in Figure 5.

Figure 7. Back-scattered electron images of composite grains of sperrylite located in the streams from Cliff.

Figure 8. Back-scattered electron images of polished sections of sperrylite and associated PGM and sulfides. (a) Elongate PtFe alloy enclosed in a broken cube of sperrylite. (b) Os-bearing ruarsite surrounded by an angular grain of sperrylite at the top and a Cu-bearing stibiopalladinite at the bottom. (c) Relicts of platarsite on the edge of an abraded sperrylite. (d) Inclusions of millerite (NiS) in sperrylite.

Figure 9. Back-scattered electron images of Pd-antimonides from the streams draining Cliff. (a-c) Pd-antimonides recovered near the disused quarries from samples C3 to C5. (a) Angular stibiopalladinite in a composite grain with a Pd-sulfide. (b) Stibiopalladinite with a ragged appearance and vast furrows on the surface. (c) Relict stibiopalladinite in a composite grain with a euhedral Pt-Pd-Cu alloy. (d-i) Pd-antimonides from further downstream to the disused quarries from samples C6 to 11. Note the extensive striation on the grain surfaces in the meander zone (d-g, samples C6 to C9) and the etched appearance with concave hollows further downstream (h-i, samples C10-C11). Pd-antimonides form composite grains with electrum in (d) and with tetraferroplatinum in (e).

Figure 10. Ternary diagrams (at.%) showing the composition of PGM from chromitites *vs.* streams at Cliff, Shetland Ophiolite Complex. (a) Pd–Sb–Cu ternary plot showing the composition of Pd-antimonides and Pt-alloys. Ideal phases within the Pd–Sb system are those reported by Kim and Chao (1991). (b) Ru–Os–Ir and Rh–Pt–Ir ternary plots showing the composition of laurite and sulfarsenides, respectively.

Figure 11. Back-scattered electron images of sulfarsenides located in the streams from Cliff. (a) Aggregate of irarsite (IrAsS) grains with altered and pitted surface. (b) Single grain of irarsite with an etched appearance. (c) The only composite grain of irarsite and

hollingworthite (RhAsS) found in the streams. Hollingworthite surrounds irarsite in the core. (d) Single grain of hollingworthite, subhedral and largely altered on surface. (e) Composite grain of hollingworthite and Pd-antimonide. (f) Composite grain of hollingworthite and a subhedral Cu-Pt-Pd-bearing particle of gold.

Figure 12. Back-scattered electron images of gold grains in the stream from Cliff (a-d) and from Harold's Grave (e-f). (a) Irregular grain of electrum located close to the Cliff quarries. (b) Subhedral grain of pure gold with a very pitted surface located downstream, in the meander zone. (c) Rounded and polished grain of electrum downstream. (d) Porous grain of electrum with a delicate texture. (e, f) Globular grains of pure gold from the alluvial sands at Harold's Grave.

Figure 13. Back-scattered electron images of gold and rare PGM in the source rocks. (a, b) Rounded porous primary Au, similar to the detrital electrum found in the placers. (c) Pt-Cu-Ni oxidised phase. (d) Pd-Cu-Ni oxidised phase on the edge of sperrylite and in stringers extending from the sperrylite. (e) Sperrylite and Pd antimonide with Cu both broken by chlorite laths. Sperrylite is partially altered to a Pt-Cu-Ni-oxide. (f) Breithauptite (NiSb) containing approximately 1 % Pd coated on the edge by Pd antimonide which contains a small grain of geversite (Pt-Sb). These altered PGE-bearing phases (c-f) are all absent in the placer assemblage.

# **Table Captions**

Table 1. Types of PGM in the Cliff chromitites and alluvial PGM recovered from the associated streams. *Footnote:* PGM in the source rocks from Prichard et al. (1986) and Prichard & Tarkian (1988) for comparison purposes.

945

946 Table 2. Types of PGM in the Harold's Grave chromitites and alluvial PGM recovered from  
947 the associated streams. *Footnote:* PGM in the rocks are from Tarkian & Prichard (1987).

948

949 Table 3. Quantitative EDX analyses of alluvial PGM from Cliff.

0°49'58"W

2 km

Unst

Loch of  
Cliff

Fig.2

Haroldswick

60°47'15"N

Cliff

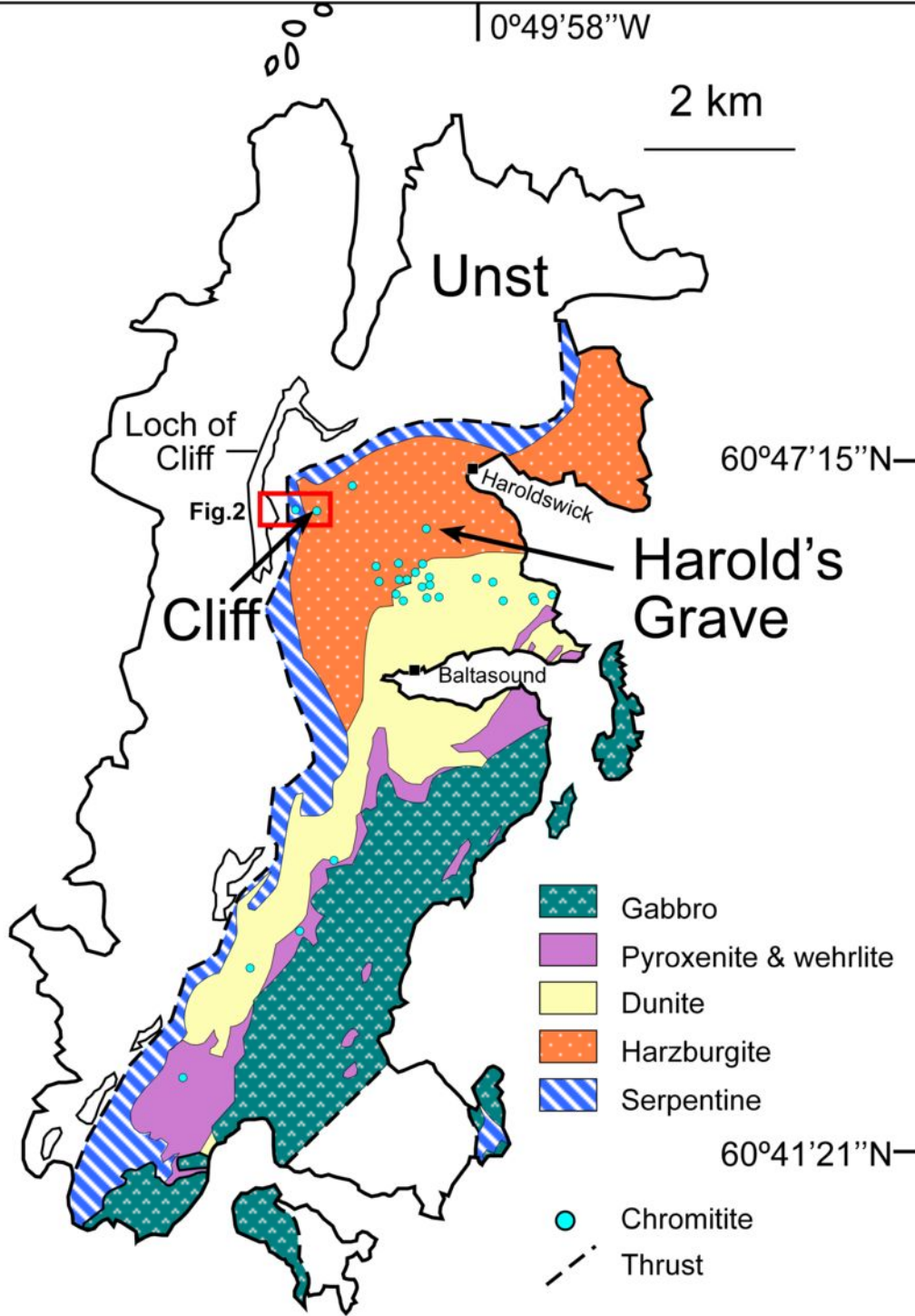
Harold's  
Grave

Baltasound

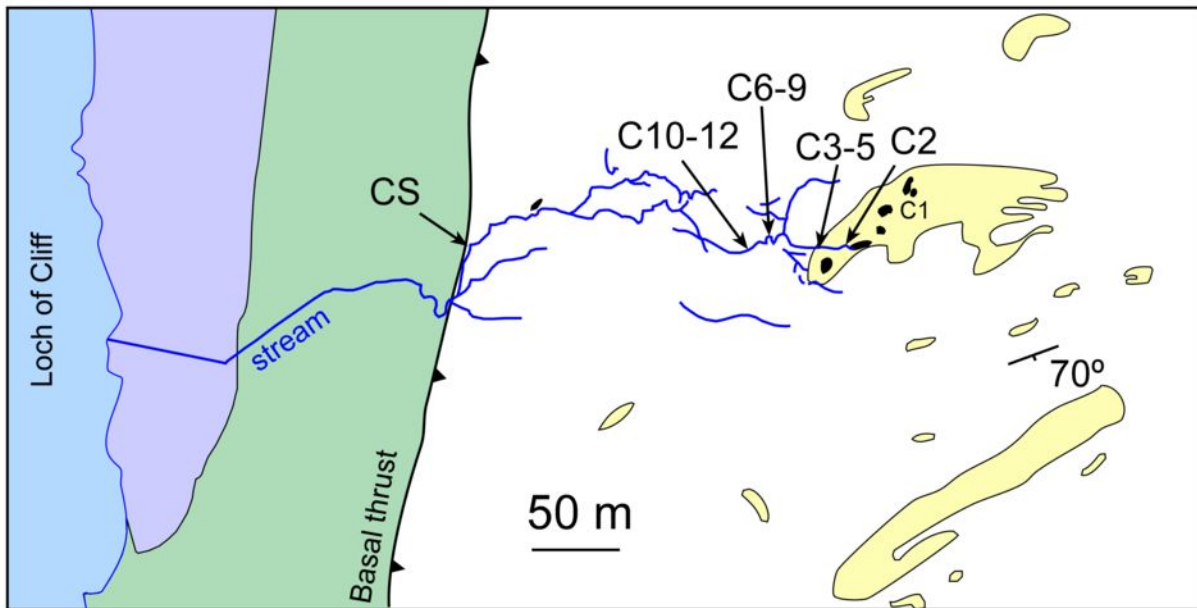
- Gabbro
- Pyroxenite & wehrlite
- Dunite
- Harzburgite
- Serpentine

60°41'21"N


- Chromitite
- Thrust



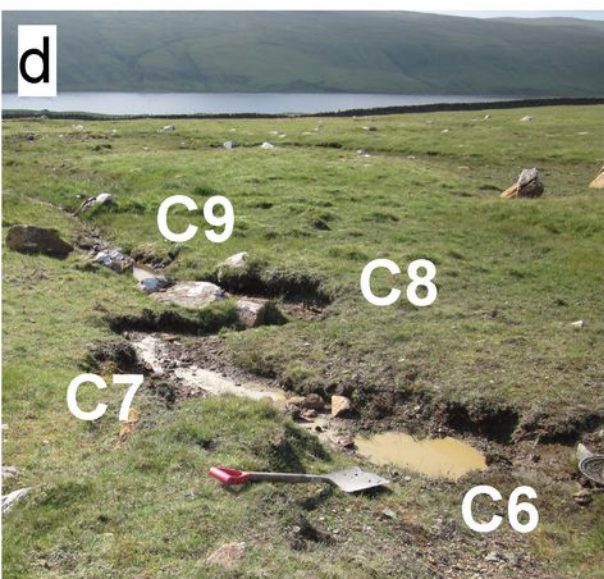
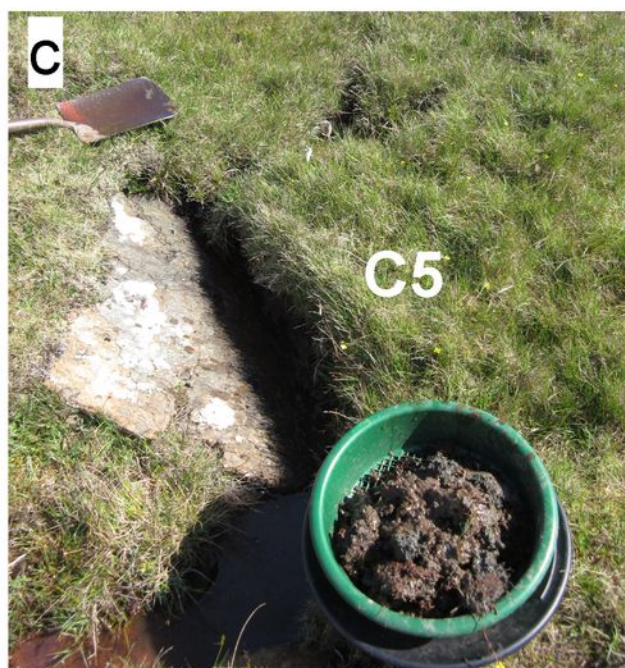
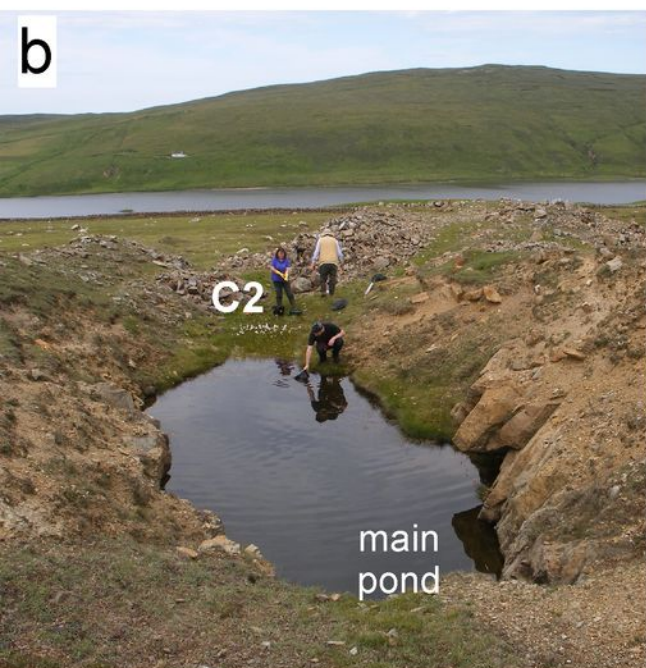
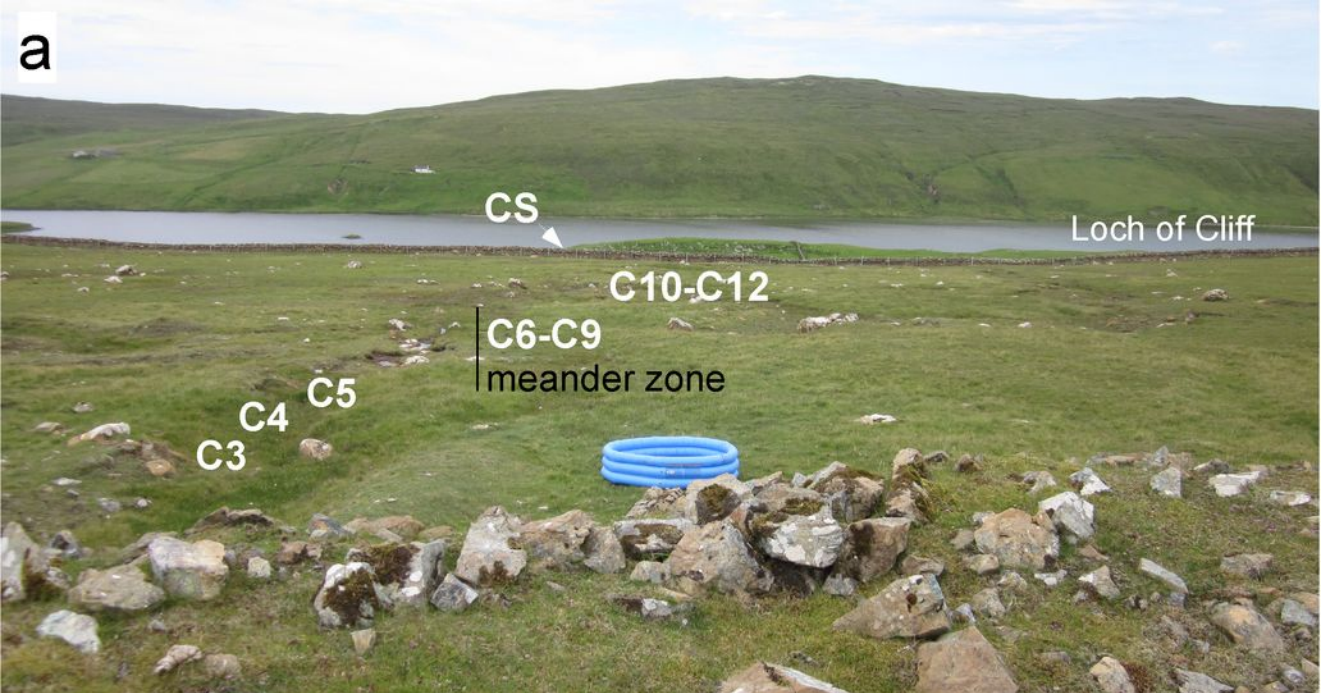




Harzburgite
  Dunite
  Chromite
  Greenschist
  Limestone

 70° foliation

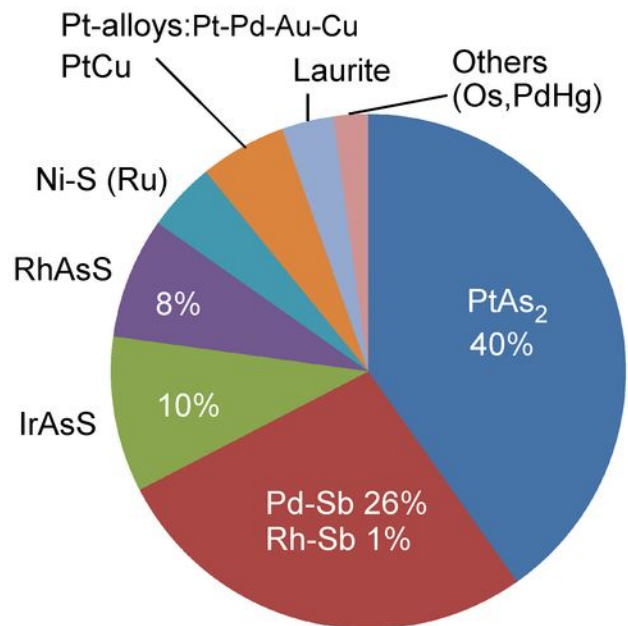






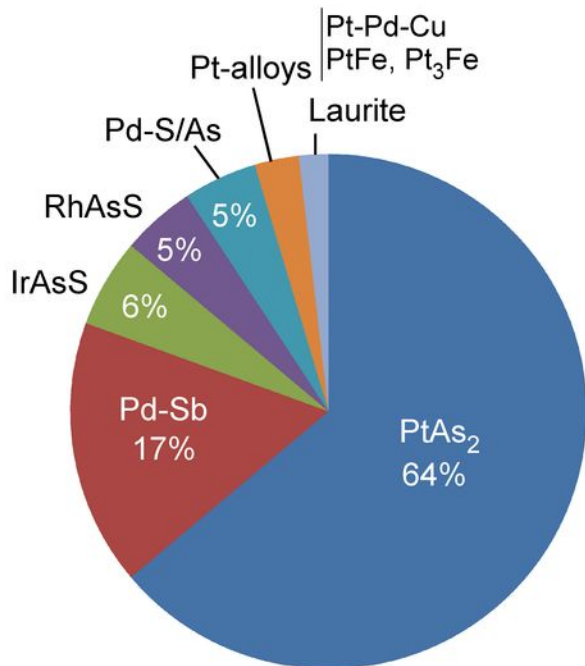
# a PGM from Cliff

## PGM in the rocks



n grains= 92 PGM + 5 Au  
(bibliographic data)

## Alluvial PGM



n grains= 108 PGM + 8 Au  
(this study)

# b

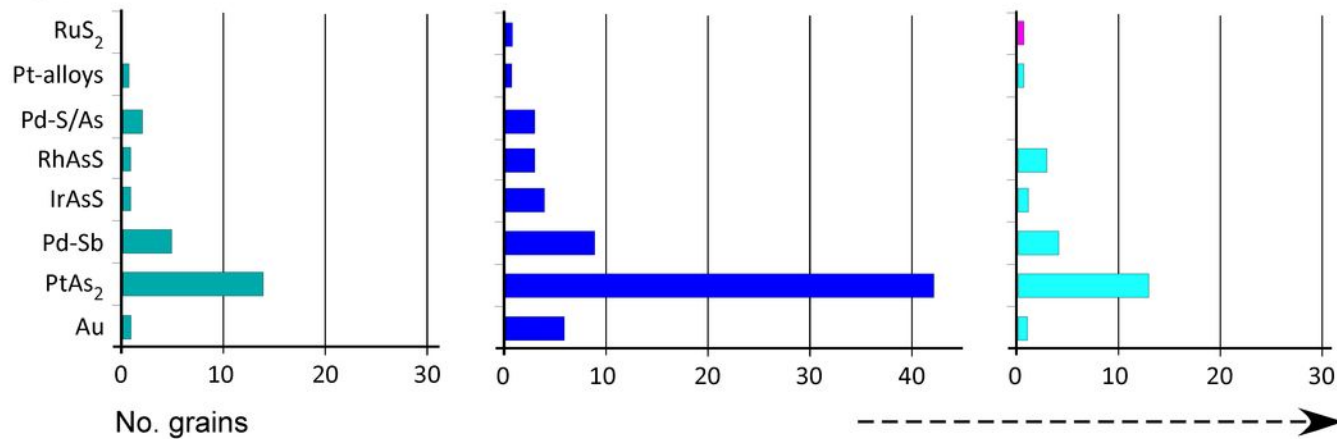
Pond exit

Meander

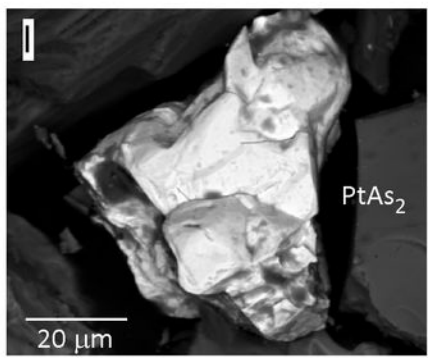
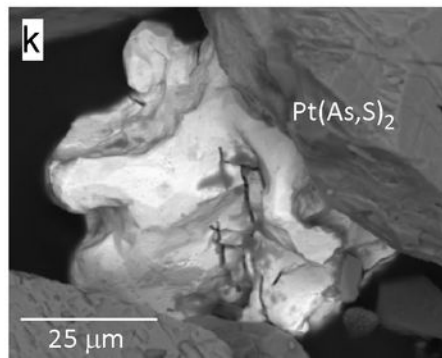
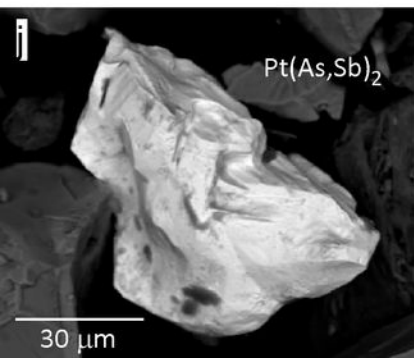
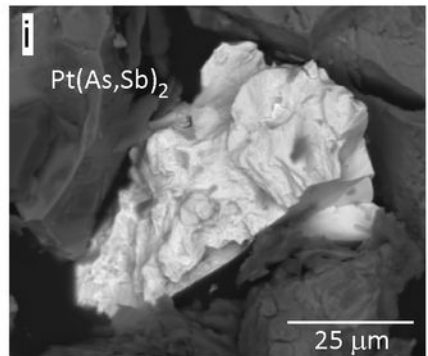
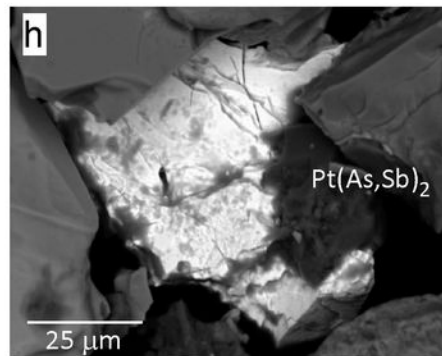
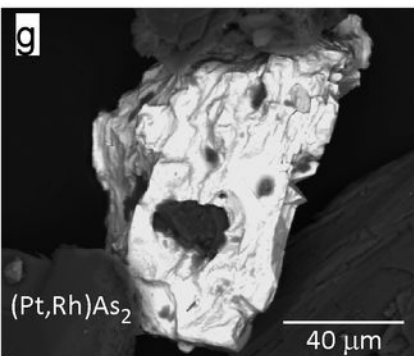
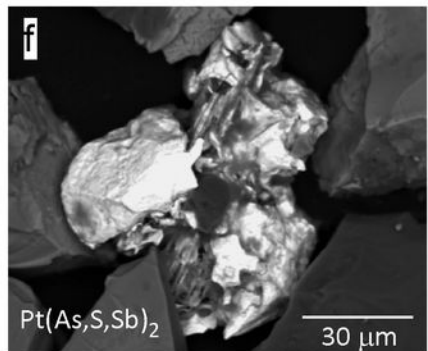
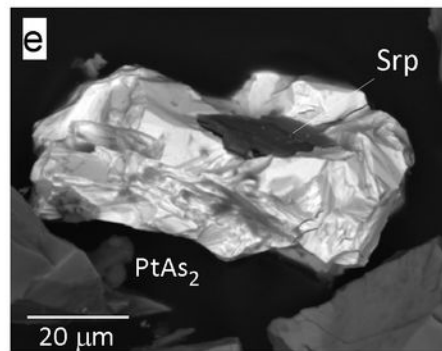
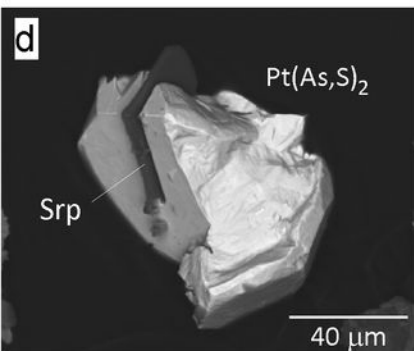
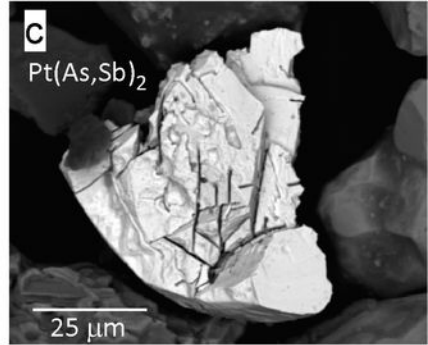
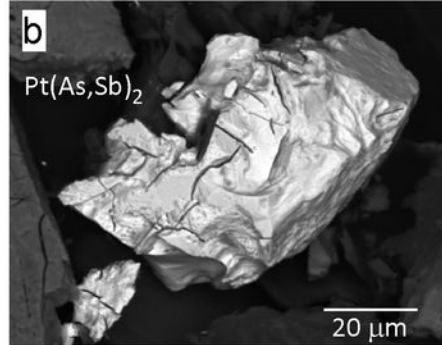
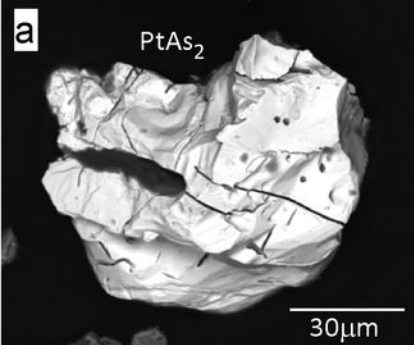
Downstream

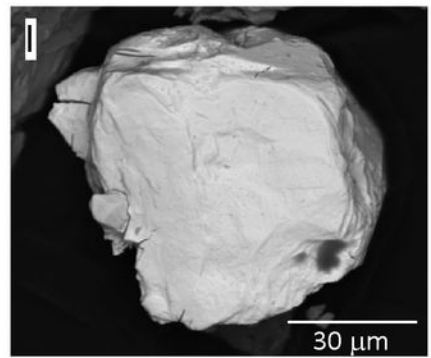
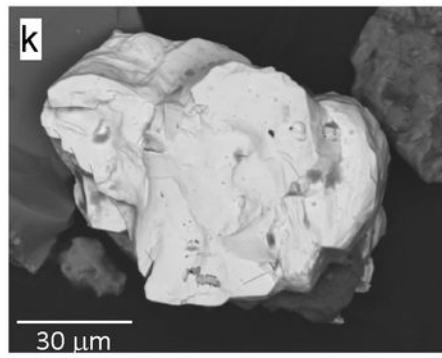
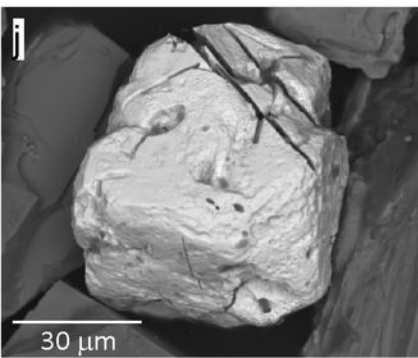
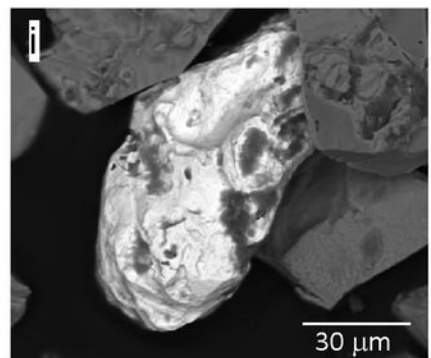
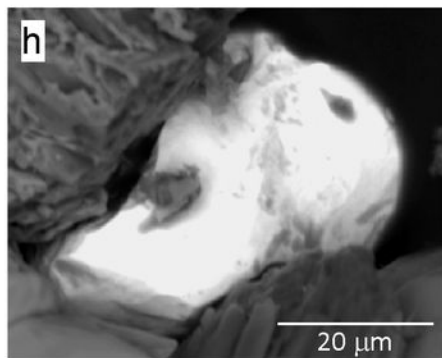
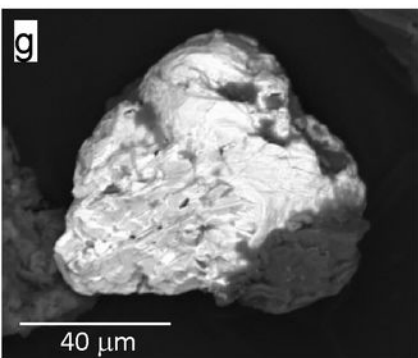
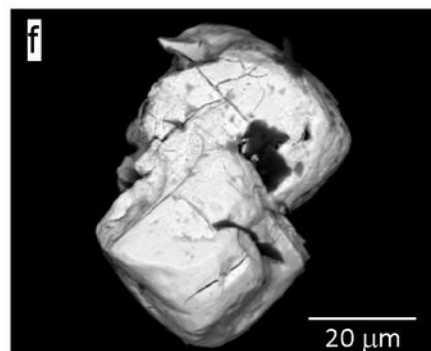
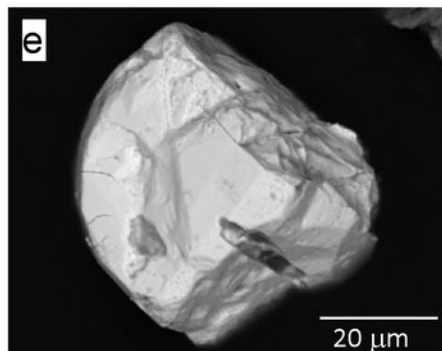
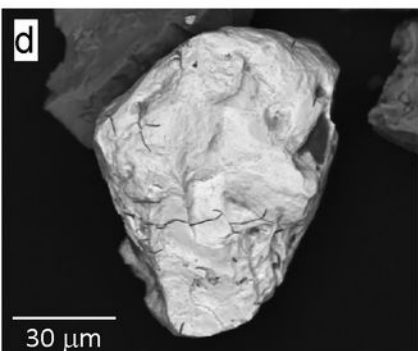
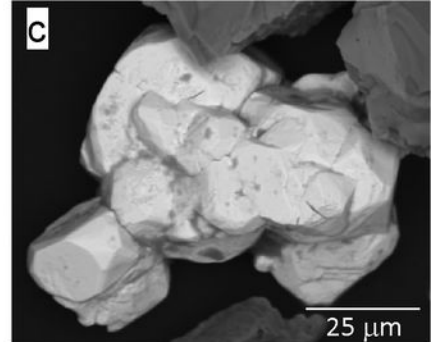
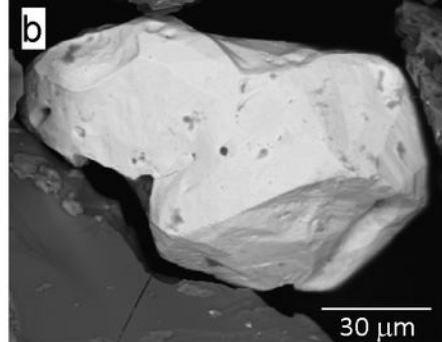
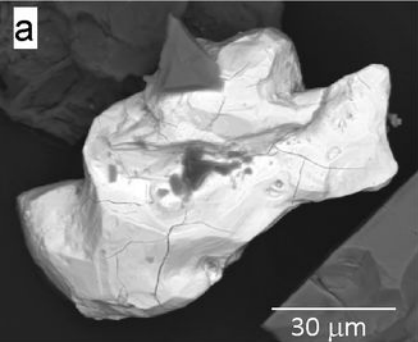
Thrust

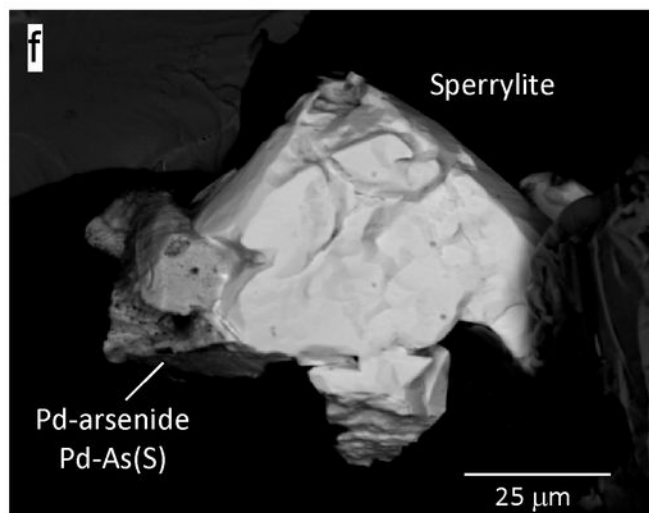
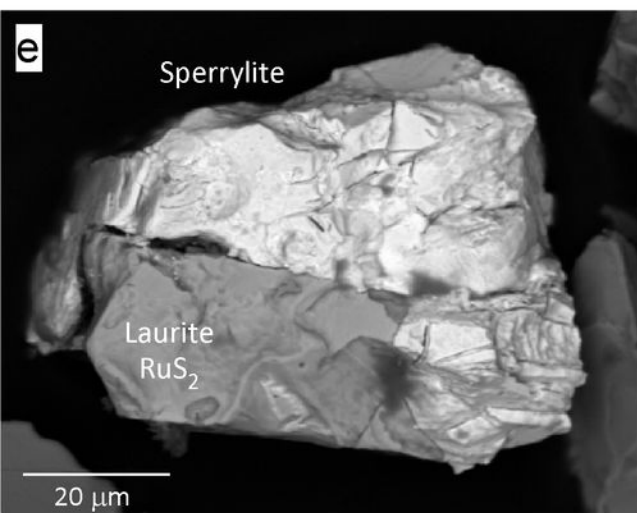
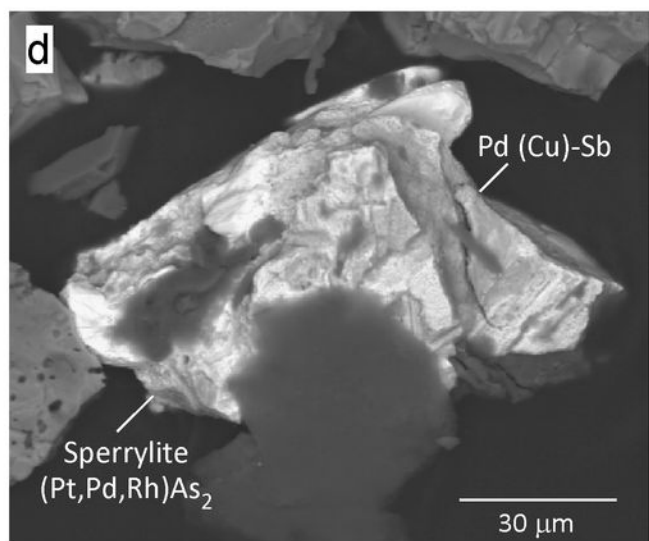
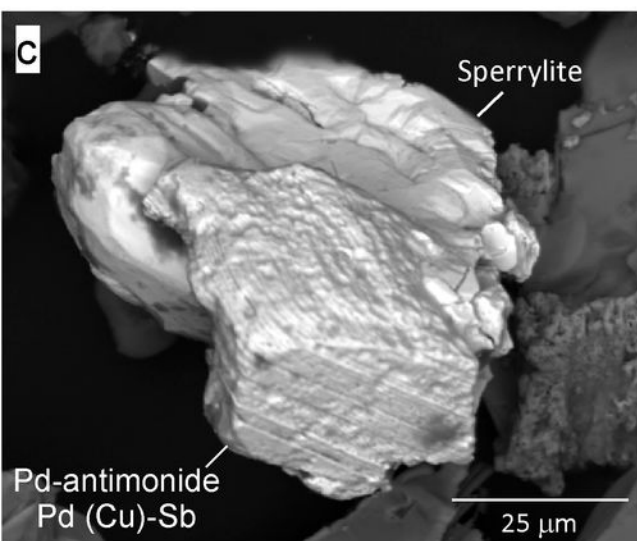
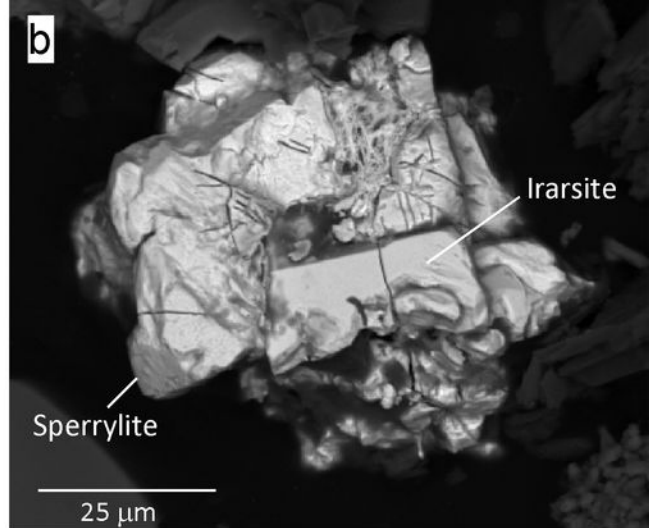
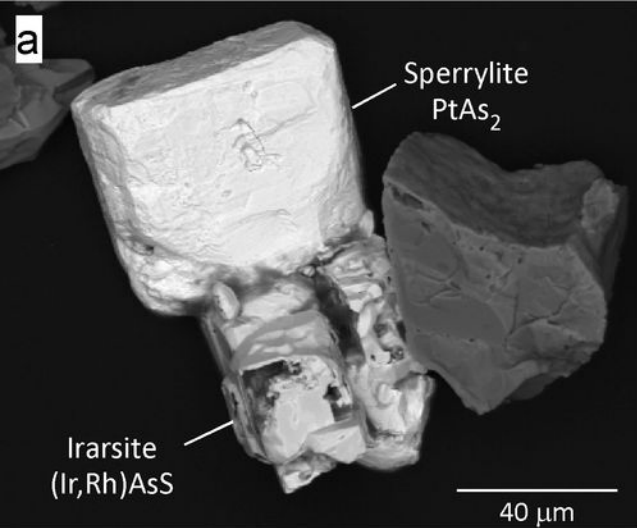
PGM

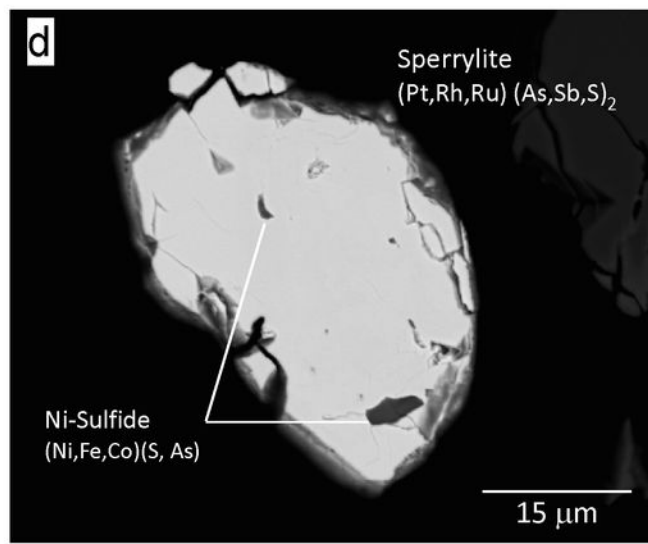
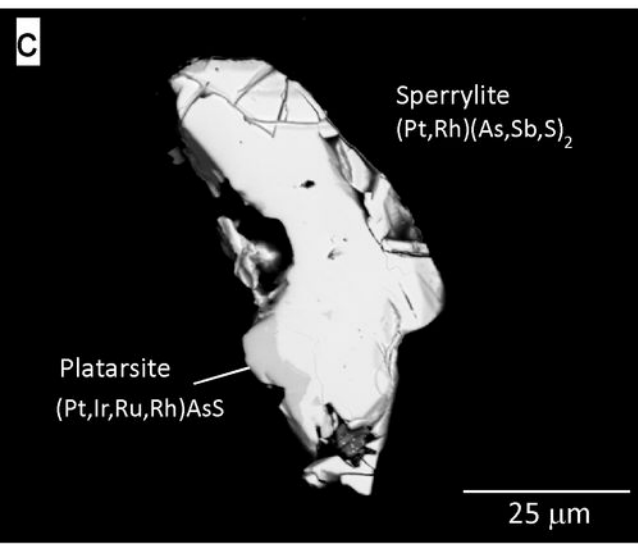
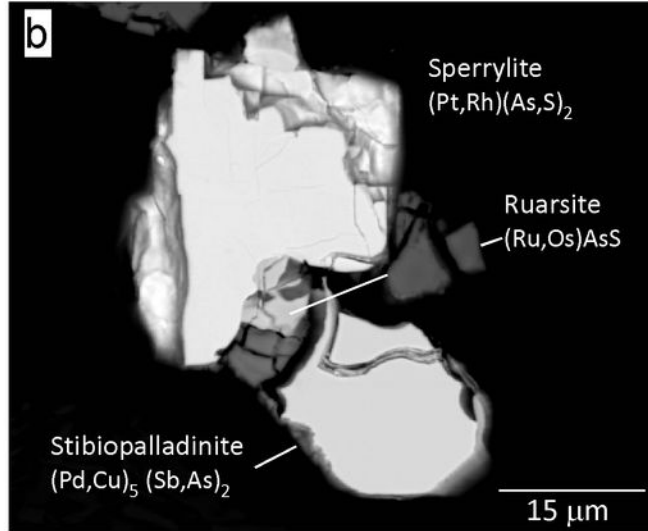
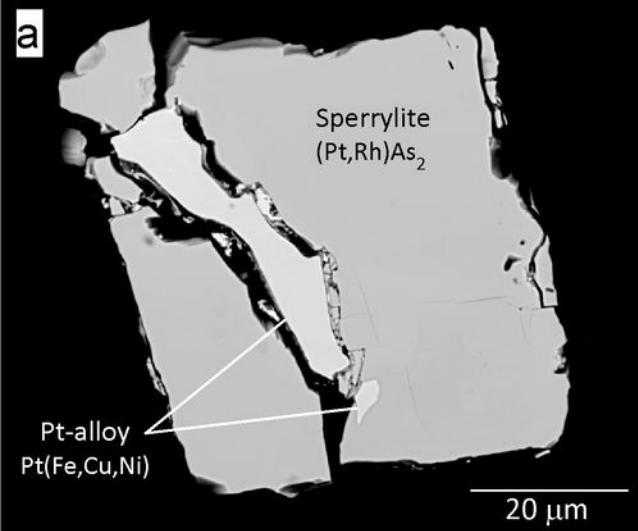


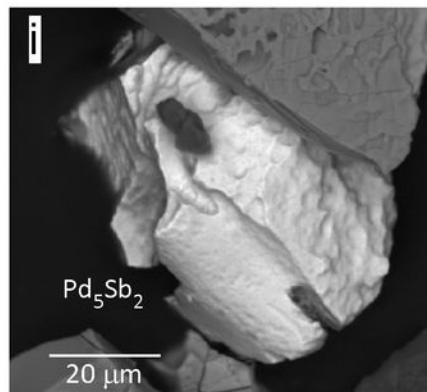
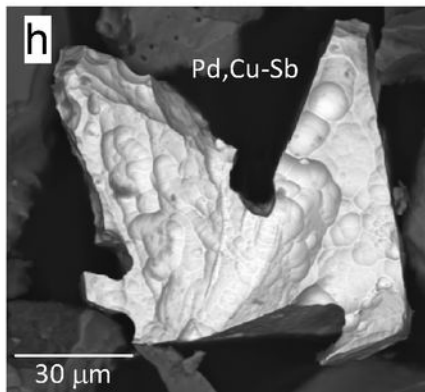
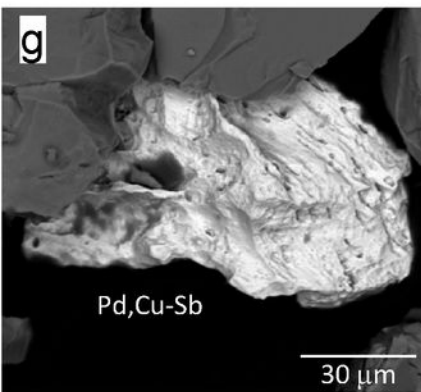
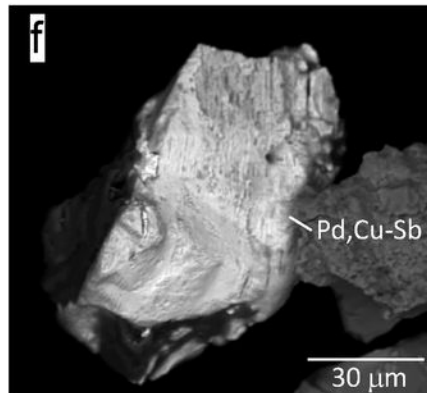
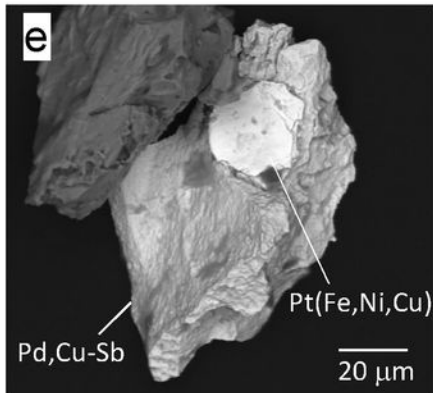
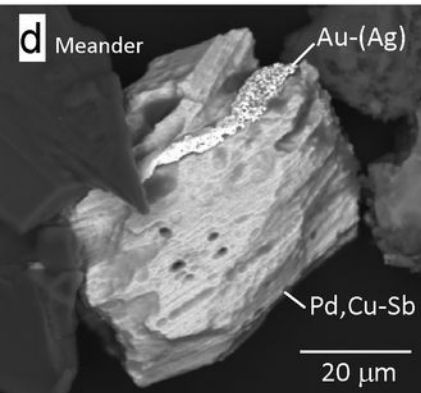
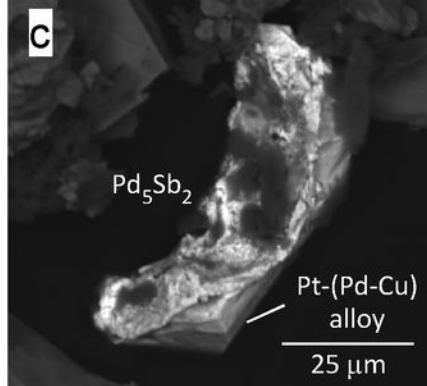
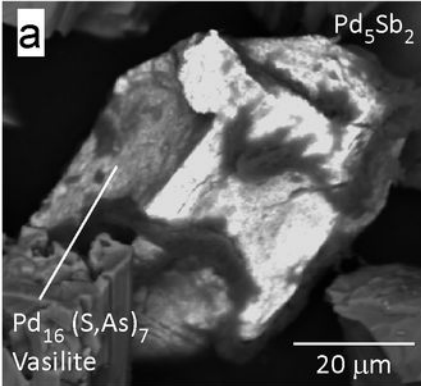
> Distance from the quarries



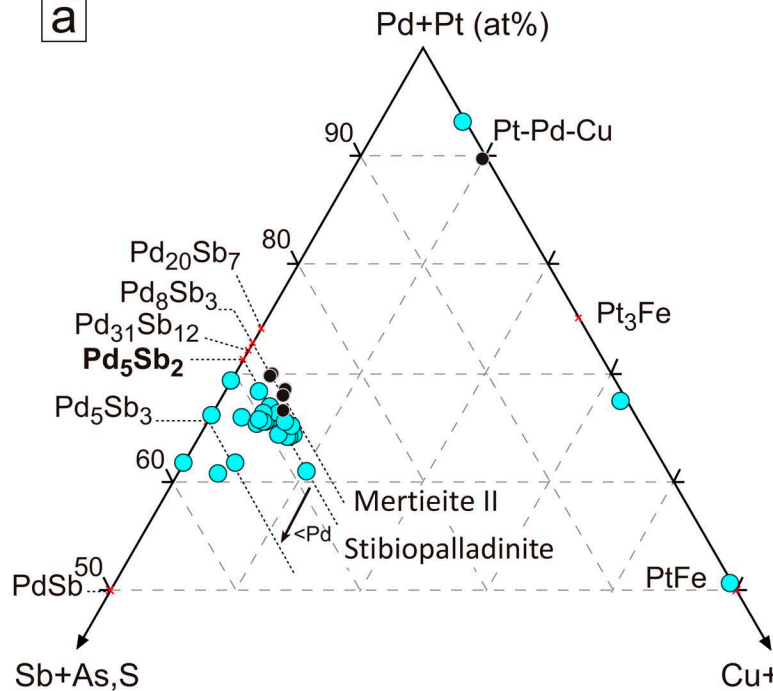
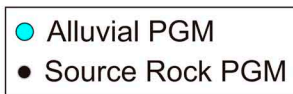
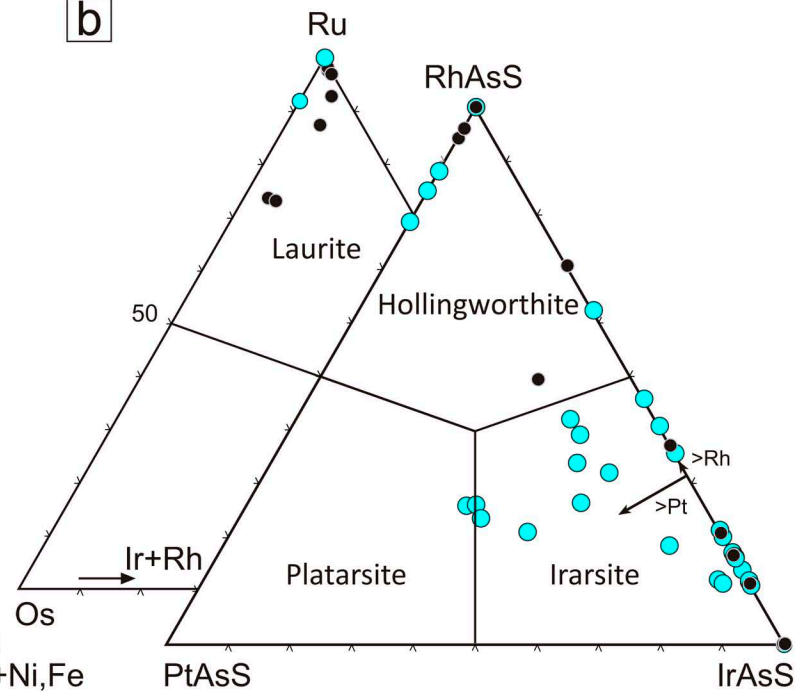


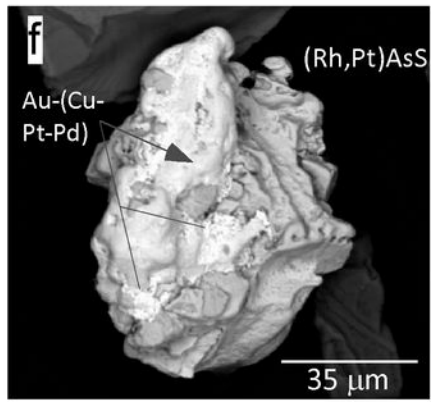
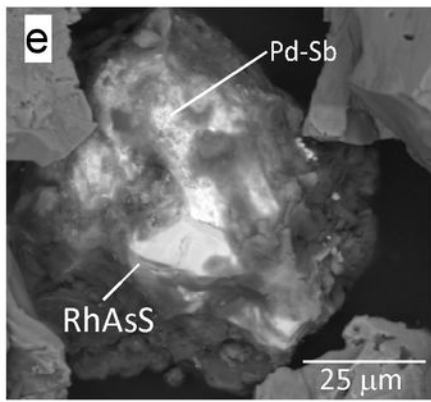
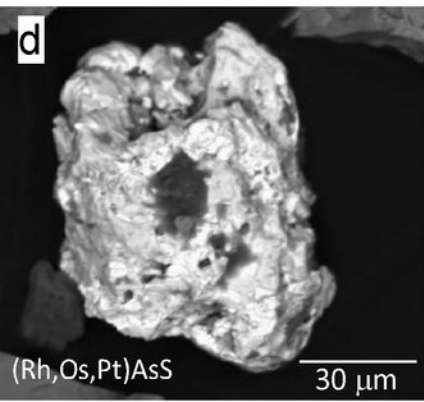
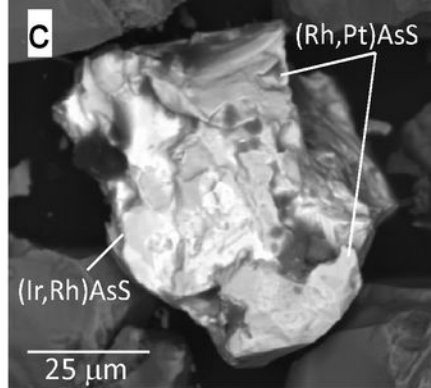
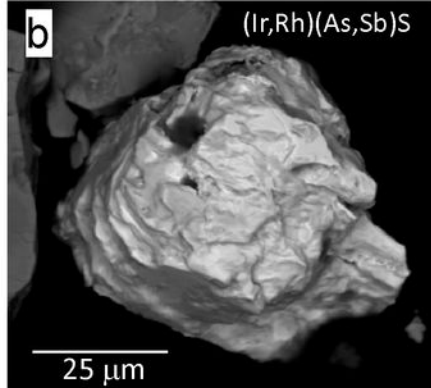
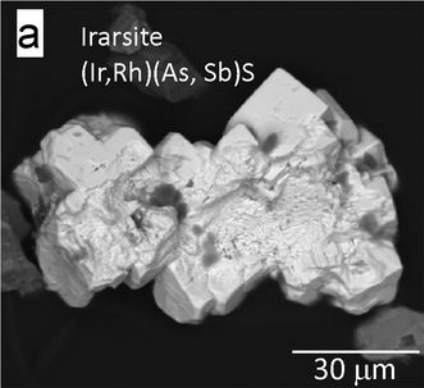


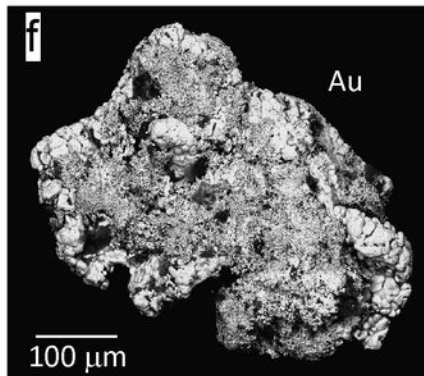
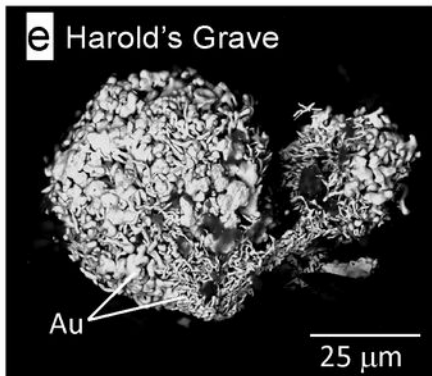
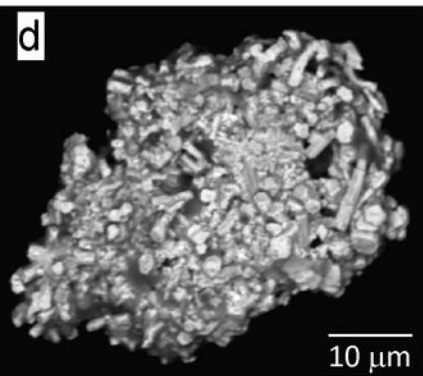
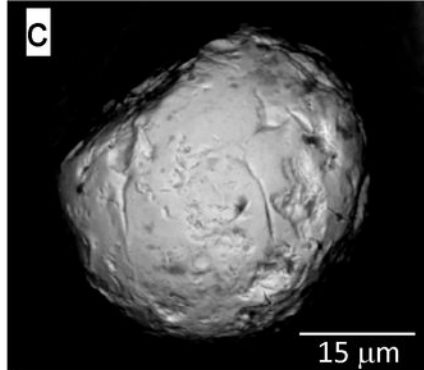
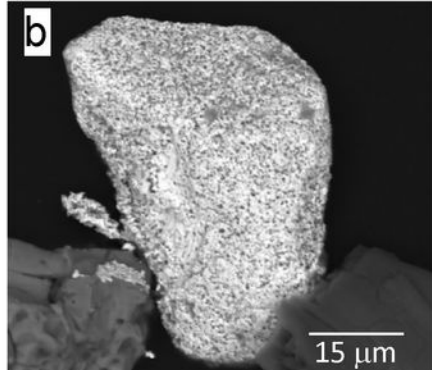
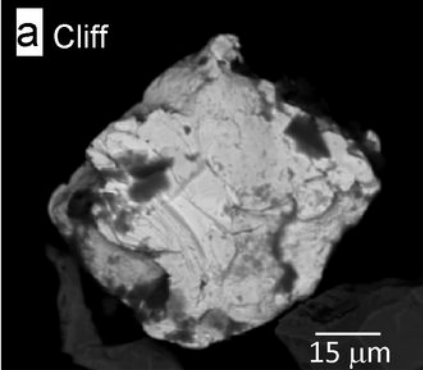






**a****b**





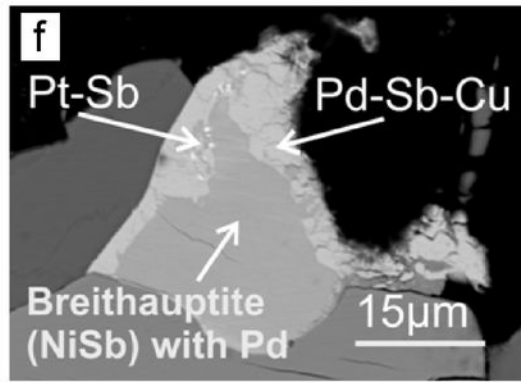
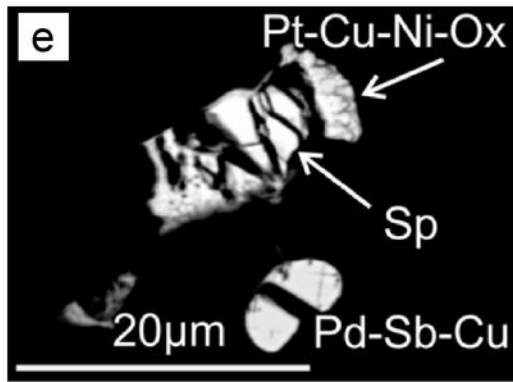
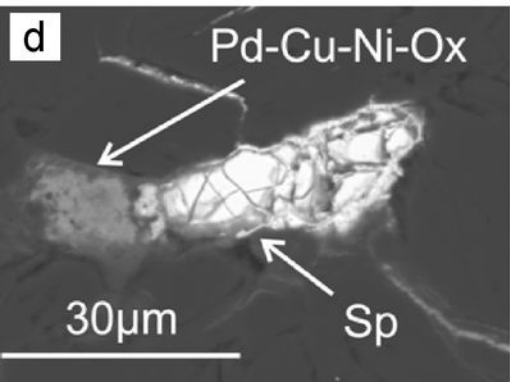
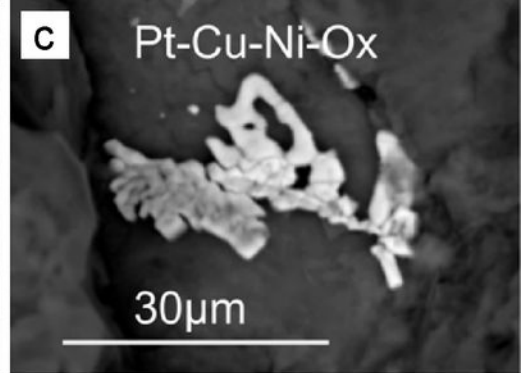
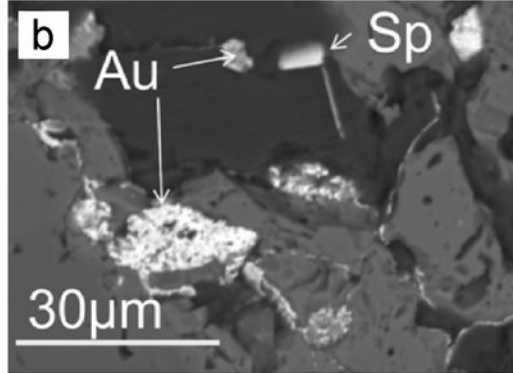
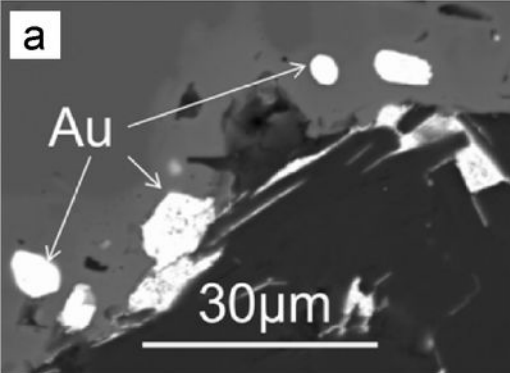


Table 1. Types of PGM in the Cliff chromitites and alluvial PGM recovered from the associated streams.

<b>1) Source Rock*</b>		No.		~Size (µm)		<b>3) Meander (samples C6-C9)</b>		No.		Size (µm)	
PGM, Au	Composition	grains	%	Min	Max	PGM, Au	Composition	grains	%	Min	Max
Sperrylite	(Pt,Fe)(As,Sb) <sub>2</sub>	37	38.1	4	20	Sperrylite	(Pt,Rh)(As,Sb) <sub>2</sub>	42	60.9	30	110
Hongshiite	PtCu+(Ni-Cu)	1	1.0	4	5	Pt-alloys	Pt (Fe,Ni,Cu)	1	1.4	15	20
Pt-alloys	Pt-Pd-Au-Cu; Pd-Cu	4	4.1	2	8	Pd-antimonide	(Pd,Fe,Cu) <sub>5</sub> (Sb,As,S) <sub>2</sub>	9	13.0	34	85
Pd-antimonide	Pd <sub>5</sub> Sb <sub>2</sub> —Pd <sub>11</sub> Sb <sub>4</sub>	24	24.7	4	17	Pd-arsenide	(Pd,Fe,Ni) <sub>2</sub> (As,S)	1	1.4	15	20
Ni-(Ru)-sulfide	(Ni,Fe,Ru,Cr) <sub>9</sub> S <sub>8</sub>	4	4.1	10	30	Pd-sulfide	(Pd,Pt,Ni,Fe)S	2	2.9	13	70
Potarite	PdHg	1	1.0	2	3	Irarsite	(Ir,Rh,Pt)AsS	4	5.8	44	63
Irarsite	IrAsS	9	9.3	10	60	Hollingworthite	(Rh,Pt)AsS	3	4.3	10	80
Hollingworthite	RhAsS	7	7.2	7	19	Laurite	RuS <sub>2</sub>	1	1.4	20	45
Rh-antimonide	Rh-Sb-S	1	1.0	3	4	Gold	Au-(Ag); Au-(Cu,Pt,Pd)	6	8.7	31	48
Laurite	RuS <sub>2</sub>	3	3.1	10	27	Total		69	100	24	60
Osmium	Os	1	1.0	2	5						
Gold	Au-(Pd), Au-Cu	5	5.2	3	4						
Total		97	100	5	17						
<b>2) Exit Pond (samples C3-C5)</b>		No.		Size (µm)		<b>4) Exit meander (samples C10-C11)</b>		No.		Size (µm)	
PGM, Au	Composition	grains	%	Min	Max	PGM, Au	Composition	grains	%	Min	Max
Sperrylite	(Pt,Rh)(As,Sb) <sub>2</sub>	14	56.0	14	92	Sperrylite	PtAs <sub>2</sub>	13	61.9	22	106
Pt-alloys	Pt-Pd-Cu alloy	1	4.0	10	50	Pt-alloys	Pt <sub>3</sub> (Fe,Ni,Cu)	1	4.8	57	62
Pd-antimonide	(Pd,Cu) <sub>5</sub> (Sb,S, As) <sub>2</sub>	5	20.0	19	90	Pd-antimonide	(Pd,Cu) <sub>5</sub> (Sb,S,As) <sub>2</sub>	4	19.0	36	103
Pd-sulfide	Pd <sub>16</sub> (S,As) <sub>7</sub>	2	8.0	8	20	Irarsite	(Ir,Rh)AsS	1	4.8	47	84
Irarsite	(Ir,Rh)AsS	1	4.0	27	60	Hollingworthite	(Rh,Os,Pt)AsS	1	4.8	64	80
Hollingworthite	(Rh,Pt)AsS	1	4.0	10	50	Gold	Au-(Pd)	1	4.8	5	20
Gold	Au-(Ag)	1	4.0	58	60	Total		21	100	39	76
Total		25	100	21	60						
<b>5) Waterfall (basal thrust, sample CS)</b>		No.		Size (µm)							
PGM	Composition	grains	%	Min	Max						
Laurite	(Ru,Os)(S,As) <sub>2</sub>	1	100	10	32						

\* PGM in the source rocks from Prichard et al. (1986) and Prichard & Tarkian (1988) for comparison purposes.

Table 2. Types of PGM in the Harold's Grave chromitites and alluvial PGM recovered from the associated streams.

<b>1) Source Rock*</b>		No.		~Size (µm)	
PGM	Composition	grains	%	Min	Max
Osmium	Os	49	47.6	2	5
Laurite	RuS <sub>2</sub>	30	29.1	10	250
Ni-(Ru)-sulfide	(Ni,Fe,Ru,Cr) <sub>9</sub> S <sub>8</sub>	4	3.9	10	30
Irarsite	IrAsS	5	4.9	10	60
Ir-antimonide	Ir-Sb-S	1	1.0	6	6
Hollingworthite	RhAsS	4	3.9	7	20
Rh-antimonide	Rh-Sb-S	3	2.9	2	4
	Rh-Ni-Sb	1	1.0	2	6
Hongshiite	PtCu	1	1.0	4	5
Pt-alloys	Pt-Pd-Cu	1	1.0	5	6
Genkinite	(Pt,Pd) <sub>4</sub> Sb <sub>3</sub>	2	1.9	2	12
Pd-antimonide	Pd <sub>5</sub> Sb <sub>2</sub> —Pd <sub>11</sub> Sb <sub>4</sub>	2	1.9	3	17
Total		103	100	5	35

<b>2) Stream</b>		No.		Size (µm)	
PGM—Sample	Composition	grains	%	Min	Max
Laurite (HG7)	RuS <sub>2</sub>	1	14.3	35	50
Iridium (HG7)	Ir-(Fe > S,As)	1	14.3	20	20
Osmium (HG10)	Os-(Ir-Ru)	1	14.3	30	60
Gold (HG1-2-7)	Au-Ag, Au-Cu	4	57.1	149	224
Total		7	100	59	89

\* PGM in the rocks are from Tarkian & Prichard (1987).

Table 3. Quantitative EDX analyses of alluvial PGM from Cliff.

Analysis	1	2	3	4	5	6	7	8	9	10	11	12	13
Sample Wt.%	C3	C5	C6	C9	C4	C6	C10	C6	C9	C5	C6	C10	C6
Pt	56.25	55.04	54.50	52.97					13.79	21.99		77.29	
Pd					63.20	64.13	63.78						
Rh	0.47		1.24	1.11				6.15	9.56	7.84			
Ir								55.78	36.64	20.78			
Ru		0.99	0.68	1.41						8.93	22.00		
Os											37.44		
Au													75.69
Ag													25.40
Cu					4.00	2.73	3.61					5.42	
Ni						0.60	0.59					4.72	
Fe												12.11	
S		0.32	0.49	1.23				12.95	11.56	11.95	13.35		
As	42.12	41.20	42.25	40.26				25.78	29.91	29.01	30.95		
Sb	1.23	2.29	0.92	2.86	31.80	31.89	32.49						
Total	100.07	99.84	100.08	99.84	99.00	99.35	100.47	100.66	101.47	100.50	103.73	99.54	101.1
At.%													
Pt	33.32	32.41	31.57	30.32					6.35	9.84		50.88	
Pd					64.70	65.67	64.24						
Rh	0.53		1.37	1.21				5.44	8.34	6.66			
Ir								26.43	17.11	9.44			
Ru		1.12	0.76	1.56						7.71	17.50		
Os											15.83		
Au													62.01
Ag													37.99
Cu					6.85	4.68	6.08					10.95	
Ni						1.12	1.08					10.32	
Fe												27.85	
S		1.14	1.71	4.28				36.79	32.37	32.54	33.46		
As	64.99	63.17	63.73	60.01				31.34	35.83	33.81	33.21		
Sb	1.16	2.16	0.86	2.62	28.45	28.54	28.60						
		Analysis											
Sperrylite	1	(Pt, Rh) <sub>1.02</sub> (As,Sb) <sub>1.98</sub>											
	2	(Pt,Ru) <sub>1.01</sub> (As,S,Sb) <sub>1.99</sub>											
	3	(Pt, Rh,Ru) <sub>1.01</sub> (As,Sb,S) <sub>1.99</sub>											
	4	(Pt,Rh,Ru) <sub>0.99</sub> (As,S,Sb) <sub>2.01</sub>											
Pd-antimonide	5	(Pd,Cu) <sub>5.01</sub> Sb <sub>1.99</sub>											
	6	(Pd,Cu,Ni,Fe) <sub>5</sub> Sb <sub>2</sub>											
	7	(Pd,Cu,Ni) <sub>5</sub> Sb <sub>2</sub>											
Irsarsite	8	(Ir,Rh) <sub>0.96</sub> As <sub>0.94</sub> S <sub>1.10</sub>											
	9	(Ir,Rh,Pt) <sub>0.95</sub> As <sub>1.08</sub> S <sub>0.97</sub>											
Platarsite	10	(Pt,Ir,Ru,Rh) <sub>1.01</sub> As <sub>1.01</sub> S <sub>0.98</sub>											
Ruarsite	11	(Ru <sub>0.52</sub> Os <sub>0.47</sub> )AsS											
Pt-alloy	12	Pt <sub>1.02</sub> (Fe <sub>0.56</sub> Cu <sub>0.22</sub> Ni <sub>0.20</sub> ) <sub>0.98</sub>											
Electrum	13	Au <sub>0.62</sub> Ag <sub>0.38</sub>											